April 1981 LBL-12558

TOPICS IN THE THEORY OF HEAVY-QUARK SYSTEMS

Curt Alan Flory
(Ph.D. Thesis)

Lawrence Berkeley Laboratory
University of California
Berkeley, CA 94720

This work was supported by the Director, Office of Energy Research, Office of High Energy and Nuclear Physics, Division of High Energy Physics of the U.S. Department of Energy under contract No. W-7405-ENG-48.

TOPICS IN THE THEORY OF HEAVY QUARK SYSTEMS

by

Curt Alan Flory

ABSTRACT

Due to the kinematic and dynamic simplifications possible because of the large mass of heavy quark bound states, certain properties of these systems can be quantitatively analyzed within the framework of Quantum Chromodynamics. It is clear that dimensionally the size of the bound state is proportional to the inverse quark mass, and for very heavy quarkonia the radius of the system should become smaller than that of normal hadrons. When this small system interacts with external long wavelength field quanta, the natural expansion that results is of a multipole type, analogous to the familiar multipole expansion in electrodynamics. This multipole expansion has better convergence properties than the standard perturbative treatment in certain kinematic regimes, which opens up a new area for strong interaction physics calculations. More specifically, it is ideally suited to investigate soft non-perturbative effects in QCD which appear to be so crucial to present day phenomenology and the conjectured confinement mechanism.

This work will utilize the heavy quarkonium multipole expansion to analyze several interesting processes. Chapter I is concerned with the production of heavy quarkonia from the

decay of even heavier quarkonia —— specifically the production of charmonium bound states from the decay of the T(9.4). Chapter II contains a calculation of F meson production in e^+e^- annihilation. Chapter III and IV are both concerned with the inclusion of non-perturbative effects in the heavy quark potential using multipole techniques. The long wavelength non-perturbative vacuum gluon condensate of Shifman, Vainshtein, and Zakharov is used to first determine when the perturbative 1/R potential for ultra-heavy quarkonia breaks down, and then to actually calculate the complete heavy quark potential out to a distance of roughly a fermi. This generates a potential which goes like 1/R at short distances, and becomes linear in R at large distances with a calculable coefficient which is in spectacular agreement with phenomenologically conjectured potentials.

Dedicated to

Teresa R. Chun

and

in memory of

Mrs. Irene Flory

Acknowledgments

I have been fortunate to have done my research at Lawrence Berkeley Laboratory during the past three and a half years. My thanks go out to all who have made it such a stimulating environment for physics. In particular I would like to thank my thesis advisor, Mchiko Suzuki, for his constant availability and insightful instruction, both individually and in the classroom. Bob Cahn also has my deep gratitude for advice and encouragement at critical times. Also, it is a pleasure to acknowledge innumerable conversations with Alan Axelrod, Neil Fleishon, Ian Hinchliffe, and Jon Sheiman that contributed greatly to my growth as a physicist.

Personal thanks go out to friends who have made the last few years in the area so enjoyable —— Bruce and Rita Armstrong, Barb Bishop, Dan Carl, Scott Friedman, John and Laura Griffin, John and Ann Hankerson, and Peter Hislop. Also, the secretaries have been friends as well as a great help in the completion of this work —— thanks are expressed to Betty A. Sublett, and Luanne Neumann and Susan Overacker who patiently typed this thesis.

Last, but certainly not least, I thank my fiancée and love of my life, Teresa Chun, for sharing this experience with me.

TABLE OF CONTENTS

Introduction

The discovery of the ψ in the fall of 1974 [1] marked the beginning of a new way to study the strong interactions. The ψ is interpreted to be the bound state of a heavy quark and its antiquark, with the new quark flavor, called charm [2], adding a new quantum number to the "old" hadron spectroscopy. The addition of another quantum number, or degree of freedom, to hadronic states was in itself not so exciting. The excitement was generated by the fact that the mass of this new quark is roughly 1.5 GeV, which is large when compared to typical masses of the strong interactions. While the old mesons suffered from the fact that the bound state quarks are extremely relativistic (i.e. mass differences on the order of the masses themselves), it was conjectured that these heavy objects within the bound state might be moving slowly, and the powerful methods for studying non-relativistic systems might be relevant. The fact that the low-lying charm-anticharm quark bound state has a mass of roughly 3.1 GeV, and the threshold for producing a charm-anticharm pair that separates and fuses with light quarks is only about .6 GeV higher indicates that the $c\bar{c}$ pair is indeed "loosely held" in the bound state and perhaps non-relativistic. Subsequent calculations of the charmonium spectrum using non-relativistic potential models have had remarkable success, and the physical picture of loosely bound, slowly moving heavy quarks is believed to be accurate. Further verification of this interpretation was obtained with the discovery of a still heavier quark bound state, called bottomonium, in the spring of 1977 [3]. This bottom-antibottom quark bound state is believed to be even more non-

relativistic than charmonium, and an even better laboratory for these techniques.

Besides the kinematic simplification that occurs due to the heavy quarks being non-relativistic, there is also a dynamic simplification that the large quark mass induces. This dynamic simplification is dependent upon a property of the currently conjectured theory of quark dynamics (i.e. strong interactions) called Quantum Chromodynamics (QCD) [4]. QCD is a nonabelian gauge field theory of the interactions of "colored" quarks and eight self-interacting (color charged) massless vector gauge bosons, the gluons. An interesting property of this theory is asymptotic freedom [5], which very simply and qualitatively stated is that the effective coupling constant of the theory becomes smaller as the invariant mass of the fundamental particles involved in the interaction process becomes larger. The hope then becomes that these heavy quarkonia states will lend themselves to sensible perturbative expansions since the coupling constant of QCD, α_s, is a reasonably small expansion parameter for sufficiently heavy states.

While the conjecture that the heavy quarkonia are non-relativistic bound states has been verified and exploited, the hope of doing simple computations as a perturbative expansion in α_s has met with serious problems. Most notably, the calculation of the first non-leading contribution in α_s for the strong decay of pseudoscalar quarkonium exhibits a breakdown in the perturbative approach [6]. The problem is that even for the heaviest quarkonium states presently accessible, the T family, the first order radiative corrections appear to be at least 50% of the lowest order annihilation term. This is a subtraction scheme dependent result but appears to remain

a problem in any scheme. It appears that α_s is not yet small enough at these mass scales to counterbalance the large coefficients in the perturbative expansion. Thus, it appears that asymptotic freedom cannot be exploited for these heavy systems, and our "perturbative hands are tied."

The lack of a naive perturbative expansion for coupling external gluons to a quarkonium bound state is not an insurmountable problem. Another property of the large quark mass can be used to advantage. It is clear that dimensionally the size of the bound state is proportional to the inverse of the quark mass (the constant of proportionality includes powers of the coupling constant). For heavy mass quarkonia, the radius of the system should become smaller than that of normal hadrons. If this small system interacts with long wavelength probes, the natural expansion that results is of a multipole type. Intuitively, there is a qualitative analogue in the coupling of neutral atoms to long wavelength external photons in QED. The expansion parameter for that process changes from the naively expected α_{EM} to $\alpha_{EM}(\underset{\sim}{k} \cdot \underset{\sim}{r})^2$, where $\underset{\sim}{k}$ is the 3-momentum of the external photon and $\underset{\sim}{r}$ is the separation vector of the atomic constituents. For soft photons ($\lambda \gg r$), the expansion parameter $\alpha_{EM}(\underset{\sim}{k} \cdot \underset{\sim}{r})^2 \ll \alpha_{EM}$, and the expansion is much better than naively expected. The origin of the additional suppression factor of $(\underset{\sim}{k} \cdot \underset{\sim}{r})^2$ is that the long wavelength probe (photon) sees a very close pair of opposite charges, both of which it couples to. A partial cancellation occurs when both couplings are summed, and the remaining contribution is due to the photon field not being homogeneous over the size of the atom, i.e. the neutral atom only couples to gradients of the

external photon field, which are proportional to powers of the 3-momentum for free fields. For QCD we can investigate a similar kinematic regime where long wavelength gluons are coupled to small color singlet quarkonia, and naively hope to improve our expansion parameter from α_s to $\alpha_s(\underline{k} \cdot \underline{r})^2$ via the same type of physical mechanism as above, and thus have a reliable methodology for a class of strong interaction calculations.

There are differences between QCD and QED which make this program somewhat difficult to implement. The complications stem from the fact that QCD is a non-abelian gauge theory, which means that the gauge fields are themselves charged and thus couple to one another. This complicates the problem of finding the gauge invariant effective multipole interaction for the following reason. All diagrams must be summed to each order in perturbation theory to have a gauge invariant set. For QED, the complete set of diagrams for coupling a photon to an atomic system bound by the one photon exchange potential is given by Fig. 1. For QCD however, the complete set of diagrams for coupling a gluon to a quarkonium system bound by the one gluon exchange potential is given by Fig. 2. It is fig. 2C that causes complications and is a manifestation of the non-abelian nature of QCD. We can see that the derivation of the QCD multipole expansion appears to depend critically upon the form of the binding potential of the quarkonium system, since the external field actually couples to the bound state exchange quanta.

Another complication that arises in the non-abelian case is due to the fact that coupling of the color singlet quarkonium to an external gluon field changes the bound state color charge — it changes

from a color singlet to a color octet. The $Q\bar{Q}$ state in a color octet is radically different from the color singlet state. For the calculable one gluon exchange potential, the color singlet is in an attractive channel and the color octet is repulsive. Furthermore, it has been conjectured that only color singlet hadronic states even exist asymptotically. Thus, a color singlet $Q\bar{Q}$ state that couples to an external gluon as in Fig. 1 becomes a highly virtual color charged octet state and must couple again to an external gluon field to color neutralize. This is illustrated in Fig. 3. Thus, the QCD multipole expansion would appear to be quite different from that of QED, i.e. the color singlet bound state must couple to more than one external gluon field to return to an asymptotic color singlet state, and these gluon-quarkonium couplings are tightly localized about the color octet intermediate states due to the octet states' high virtuality [7].

Even with these complications as mentioned above, a multipole expansion for the soft gluon-heavy quarkonium coupling can be derived [7], [8]. The expansion has the basic properties that were physically motivated previously using the QED analogue, i.e. the expansion parameter has very roughly been improved from α_s to $\alpha_s(\underset{\sim}{k}\cdot\underset{\sim}{r})^2$. This opens up a new region for reliable strong interaction calculations which have a well behaved series expansion. Not only does it make possible certain straight perturbative style calculations, but it also allows one to get a handle on the soft non-perturbative effects in QCD which appear to be so crucial to present day phenomenology and the conjectured confinement mechanism.

The effective interaction Lagrangian for the QCD multipole expansion which will be exploited throughout this work has the form

$$\mathcal{L}_I = \sum_a [- Q_a A_a^0(0,t) + \underset{\sim}{d}_a \cdot \underset{\sim}{E}_a(0,t) + \underset{\sim}{m}_a \underset{\sim}{B}_a(0,t) + \ldots]$$

where

$$Q_a = g \int d^3r \; \psi \gamma_0 T_a \psi$$

$$d_a = g \int d^3r \; \underset{\sim}{r} \bar{\psi} \gamma_0 T_a \psi$$

$$m_a = g \int d^3r \; \frac{1}{2} (\underset{\sim}{r} \times \bar{\psi} \underset{\sim}{\gamma} T_a \psi)$$

with ψ the $Q\bar{Q}$ wavefunction, $\underset{\sim}{r}$ the $Q\bar{Q}$ separation, and T_a the generators of $SU_c(3)$. The explicit form of the dipole couplings will be derived in Chapter I, and then used in later chapters. When higher order multipoles are necessary to estimate neglected terms, we will directly use the results of Ref. 8.

In this thesis, several topics which have the unifying thread of utilizing the soft gluon-heavy quarkonium coupling will be investigated. Chapter I [9] is concerned with the production of heavy quarkonia from the decay of even heavier quarkonia — more specifically the production of charmonium bound states from the decay of the T(9.4). The soft gluon-heavy quarkonium coupling is needed due to the fact that for this process, the charmonium final state is produced from a single (color octet) gluon and must radiate another (soft) gluon to color neutralize. This final state color rearrangement is shown to greatly suppress the branching ratio to charmonium. Chapter II contains a calculation of F meson production (states of net charm and strangeness) in e^+e^-

annihilation at the energy of the ψ(4414) [10]. As this energy is just above $F\bar{F}$ threshold, the soft gluon techniques are once again useful. We find that our production mechanism can account for at least a large fraction of the observed rate.

Chapters III and IV are both concerned with the inclusion of non-perturbative effects in the heavy quark potential. The general procedure is to accept the hypothesis of Shifman, Vainshtein, and Zakharov that the long wavelength non-perturbative structure of QCD can be parameterized by non-zero vacuum expectation values (VEV) of certain gauge invariant field operators [11]. The VEV's are determined from experiment, and then can be used to calculate non-perturbative effects in other processes. We use the soft gluon-heavy quarkonium coupling to incorporate the effects of these long wavelength VEV's on the heavy $Q\bar{Q}$ state. Chapter III determines when the 1/R potential, which is dominant for ultra-heavy quarkonia, breaks down due to non-perturbative effects [12]. Chapter IV is a more sophisticated calculation that actually determines the heavy quark potential out to a distance of roughly a fermi by incorporating the perturbative one gluon exchange potential and the relevant non-perturbative effects within the framework of Shifman et al.'s VEV's. The derived potential is in spectacular agreement with proviously conjectured phenomenological potentials fit to the data, and has a linearly rising confining potential with precisely the correct coefficient to reproduce the Regge slope [13].

Finally, we close with a short summary and mention possible extensions of this work.

References

1. J. J. Aubert et al., Phys. Rev. Lett. 33 (1974) 1404; J. E. Augustin et al., Phys. Rev. Lett. 33 (1974) 1406; G. S. Abrams et al., Phys. Rev. Lett. 33 (1974) 1453.
2. J. D. Bjorken and S. L. Glashow, Phys. Lett. 11 (1964) 255; S. L. Glashow, J. Iliopoulous, and L. Maiani, Phys. Rev. D2 (1970) 1285; M. K. Gaillard, B. W. Lee, and J. L. Rosner, Rev. of Mod. Phys. 47 (1975) 277.
3. S. W. Herb et al., Phys. Rev. Lett. 39 (1977) 252; W. R. Innes et al., Phys. Rev. Lett. 39 (1977) 1240; K. Ueno et al., Phys. Rev. Lett. 49 (1979) 486.
4. H. Fritzsch, M. Gell-Mann, and H. Leutwyler, Phys. Lett. B47 (1973) 365; D. J. Gross and F. Wilczek, Phys. Rev. D8 (1973) 3497; S. Weinberg, Phys. Rev. Lett. 31 (1973) 494.
5. G. t'Hooft, unpublished; D. J. Gross and F. Wilczek, Phys. Rev. Lett. 30 (1973) 1343; H. D. Politzer, Phys. Rev. Lett. 30 (1973) 1346.
6. R. Barbieri, G. Curci, E. d'Emilio, and E. Remiddi, Nucl. Phys. B154 (1979) 535.
7. M. E. Peskin, Nucl. Phys. B156 (1979) 365; G. Bhanot and M. E. Peskin, Nucl. Phys. B156 (1979) 391.
8. T. -M. Yan, Phys. Rev. D22 (1980) 1652; K. Shizuya, LBL Report No. LBL-11004 (to be published).
9. Curt A. Flory, Phys. Lett. 94B (1980) 221.
10. Curt A. Flory, Phys. Lett. 99B (1981) 365.

11. M. A. Shifman, A. I. Vainshtein, and V. I. Zakharov, Nucl. Phys. B147 (1979) 385.

12. Curt A. Flory, LBL Report No. LBL-11551, to appear in Phys. Lett. B.

13. Curt A. Flory, LBL Report No. LBL-12385, submitted to Phys. Rev. Lett.

Figure Captions

Fig. 1. Photon coupling to system bound by one photon exchange potential.

Fig. 2. Gluon coupling to quarkonium system bound by one gluon exchange potential.

Fig. 3. Quarkonium color singlet to color singlet transition via lowest order gluon emission.

FIG. 1

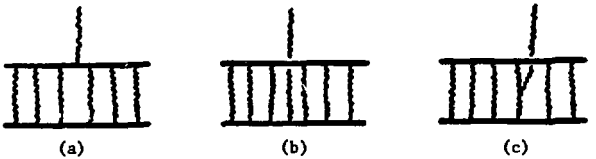

FIG. 2

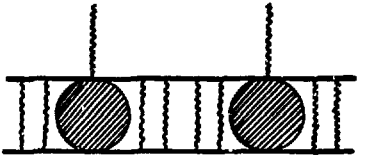

FIG. 3

CHAPTER I

Quarkonium Production Via The One Gluon Mechanism

Abstract

Using multipole techniques within the framework of Quantum Chromodynamics, it is determined that quarkonium production from a single virtual gluon is suppressed due to the lack of colored resonances. The branching ratio to charmonium in $\Upsilon(9.4)$ decay is estimated to be between 10^{-2} and 10^{-3} times smaller than previous estimates.

I. Introduction and review of previous calculations

As previously discussed, there are several powerful techniques available for dealing with heavy quark states — most notably the non-relativistic approximation and the multipole expansion. A candidate process which deals with only heavy quarks is the production of heavy quarkonia in the decay of still heavier $Q\bar{Q}$ states. Within the framework of QCD, it is supposed that a heavy quarkonium state ($J^{PC} = 1^{--}$) decays into three gluons which materialize by fragmenting into hadrons. We expect heavy flavors to be produced in this process only through a virtual timelike gluon of large invariant mass. The process is illustrated by Fig. 1.

The total rate for producing heavy flavors in the final state for this process has been estimated [1]. The estimate is based upon an analogue to electromagnetic heavy flavor production in e^+e^- annihilation. It is well known that in e^+e^- annihilation the cross section for producing a specific flavor is roughly equal to the cross section for producing a free pair of quarks, if one averages over resonance bumps [2]. This same idea of duality was applied to heavy flavor production in quarkonium decay by calculating the rate for production of a pair of free heavy quarks, as in Fig. 1. The authors of Ref. 1 thus determine the branching ratio of the $\Upsilon(9.4)$ to charm + anticharm ($c\bar{c}$) + two gluons. The branching ratio is given as a function of the dimensionless parameter ξ, which is defined as Q^2/m_T^2, where Q^2 is the invariant mass squared of the produced charm-anticharm pair. Their results are summarized in Fig. 2. The total branching ratio to charmed particles is obtained by integrating the differential branching ratio, $\rho(\xi)$, over the entire kinematic range

of ξ. To obtain partial branching ratios, one can integrate $\rho(\xi)$ just over the energy range which contains the desired final charm state.

The charmonium spectrum consists of the $c\bar{c}$ bound states $\eta_c(^1S_o)$, $\psi(^3S_1)$, and $\chi(^3P_J)$ which exist below the threshold for producing states which contain a particle with charm +1 and a particle with charm -1. These "net charm" particles consist of a charmed quark combined with a light flavor antiquark, and are called D mesons. It is assumed that when the above differential branching ratio is integrated from the minimum Q^2 up to $(2m_D)^2$, we obtain the branching ratio to find the final state charm manifesting itself as the charmonium $c\bar{c}$ bound states (η_c, ψ,χ). Furthermore, integrating $\rho(\xi)$ from $(2m_D)^2$ up to the maximum Q^2 gives the branching ratio to $D\bar{D}$ final states. The authors of Ref. 1 find branching ratios of 2.7% to $D\bar{D}$, and 1.1% to charmonium in the decay of the Υ.

II. Necessary modification of the previous result

Essential to the referenced authors' determination of the branching ratio to charmonium bound states is the assumption of duality. However, this does not seem a reasonable assumption since the produced $c\bar{c}$ pairs are not produced in a color singlet state. Since colored resonances have not been observed, one should not expect dynamical enhancement of $c\bar{c}$ production through the one gluon mechanism at discrete (bound state) energies, and thus not have an operative version of duality working. Instead, one must calculate the rate for the specific color singlet final state desired. This means that the process "g" $\rightarrow (c\bar{c})$ + g must be calculated, and then used to replace the subprocess "g" $\rightarrow c\bar{c}$ that appears in the work of Ref. 1. The modification that our work [3] incorporates is symbolically given

by Fig. 3.

The lowest order diagrams that must be calculated to obtain a gauge invariant result are those of Fig. 4. In words, they correspond to heavy quark-antiquark production via a virtual gluon, followed by propagation of the system in a color octet state, with the subsequent emission of an on-shell gluon which is coupled either directly to a quark (Fig. 4a, b) or to a virtual gluon exchanged between the quark lines (Fig. 4c). It is expected that the emitted gluon can be treated as free, since how it eventually combines with the other color octet fragments into a color singlet hadronic state should be explained by duality, i.e. it hadronizes with unit probability. The remaining quark system is then projected onto the desired color singlet state. The justification for doing a perturbative treatment of soft gluon emission is based upon our previous multipole arguments. This is a "quasi-dipole" type coupling of a long wavelength probe (gluon) to a small source (quarkonium), which conspires with limited phase space to give a small effective expansion parameter suppressing higher order soft gluon emission. For this same reason, we must restrict ourselves to final state charmonium and not $(c\bar{q})(\bar{c}q)$ final states (where q denotes a light quark).

In order to illustrate the mechanics of heavy quarkonia production and to specifically estimate the branching ratio of T to charmonium, we will assume the charm-anticharm potential is reasonably approximated by the lowest order perturbative one gluon exchange potential. This approximation should yield an order of magnitude estimate for charmonium, and will become increasingly more accurate as one deals

with heavier quark systems. In the following we will refer to the $c\bar{c}$ pair as a $Q\bar{Q}$ pair to emphasize the generality of the derived expressions.

The calculation of the relevant S-matrix element begins by adopting a modified interaction picture where the Hamiltonian is divided into an external perturbative part (H_E) which describes the coupling of the $Q\bar{Q}$ system to external gluons, and a part treated "non-perturbatively" which describes the internal interactions of the $Q\bar{Q}$ system. The internal Hamiltonian for the $Q\bar{Q}$ system in the attractive (repulsive) color singlet (octet) state is $H_1(H_8)$. The lowest order S-matrix element for the process "g" $\rightarrow \Phi + g$, where Φ generically refers to a $Q\bar{Q}$ color singlet bound state, is

$$S = -2\pi\delta(E_f - E_i) \langle \Phi\, g | \int_0^\infty dt\, H_E(t)\, \exp[-i(H_8 + \epsilon_1)t] H_E(0) | \text{"g"} \rangle \tag{1.1}$$

with ϵ_1 the binding energy of the state Φ. Inserting a complete set of intermediate color octet states and rotating to Euclidean space yields

$$S = 2\pi i\delta(E_f - E_i) \langle g\, \Phi | \int_0^\infty dt\, H_E(t)\, \exp[-(H_8 + \epsilon_1)t] | Q\bar{Q} \rangle_8 \frac{V\, d^3p_Q}{(2\pi)^3} \frac{V\, d^3p_{\bar{Q}}}{(2\pi)^3}\, {}_8\langle Q\bar{Q} | H_E(0) | \text{"g"} \rangle . \tag{1.2}$$

Note that here we see where the damping due to the octet virtuality comes in. The first matrix element in Eq. 1.2 is the difficult part

of the calculation. It contains the soft gluon-heavy quark state coupling in the form $(Q\bar{Q})_8 \to \phi g$. It's evaluation will be the topic of the next section, and we will find the beginning of the awaited multipole expansion.

III. Form of the soft gluon-heavy quarkonium coupling

To evaluate the $(Q\bar{Q})_8 \to \phi g$ matrix element we closely follow the techniques developed by Peskin [4] in deriving his operator product expansion for heavy quark systems. Due to the specific matrix element we are calculating, we shall see that the only diagrams we must calculate are those of Fig. 5. It remains to show that this is a gauge invariant set of diagrams and that all the diagrams are the same effective order in the coupling constant. Using the non-relativistic Feynman rules given in Appendix A, and restricting the emitted gluon to timelike polarization, Fig. 5a + 5b can be reduced to

$$(5a + 5b, \text{ timelike}) = -\frac{i(2\pi)^3\delta^3(P_f - P_i)}{V^{3/2}(2k_o)^{1/2}} \frac{(igT_b)_{\alpha\beta}}{\sqrt{3}} \delta_{s_1 s_1'} \delta_{s_2 s_2'}$$

$$\times \langle \Phi | [A_o^b(\tau, R + \tfrac{1}{2}r) - A_o^b(\tau, R - \tfrac{1}{2}r)] \exp[-(H_8 + \varepsilon_1)\tau] d\tau | Q\bar{Q} \rangle_8 \tag{1.3}$$

where R is the center of mass coordinates of the Φ, r is the relative quark spacing, and the A field has been made dimensionless. Furthermore, the approximation can be made that

$$[A_o^b(\tau, R + \tfrac{1}{2}r) - A_o^b(\tau, R - \tfrac{1}{2}r)] = \underset{\sim}{r} \cdot \underset{\sim}{\partial} A_b^o(\tau, R) + O(rk_o)^3$$

$$\approx \underset{\sim}{r} \cdot \underset{\sim}{\partial} \sum_{n=0}^{\infty} \frac{1}{n!} \tau^n [(\frac{d}{dt})^n A_b^o(t, R)]_{t=\sigma} \tag{1.4}$$

which neglects terms of order $(|\underset{\sim}{k}|r)^3$ and keeps all powers of (k_o/ε_1). Doing the now trivial τ integration yields

$$(5a + 5b, \text{ timelike}) = -\frac{i(2\pi)^3\delta^3(P_f - P_i)}{V^{3/2}(2k_o)^{1/2}} \frac{(igT_b)_{\alpha\beta}}{\sqrt{3}} \delta_{s_1 s_1'} \delta_{s_2 s_2'}$$

$$\times \sum_{n=0}^{\infty} <\phi|r_i \frac{1}{(H_8 + \varepsilon_1)^{n+1}}|Q\bar{Q}>_8 (\partial_o)^n (\partial^i A_o^b). \tag{1.5}$$

Note that this looks like the beginning of an electric dipole transition, i.e. the $(Q\bar{Q})_8$ state propagates via the $\frac{1}{(H_8 + \varepsilon)}$ energy denominator, then couples to $\underset{\sim}{r} \cdot \underset{\sim}{\nabla} A_o$, with an outgoing gluon and $(Q\bar{Q})_1$ final state. The expression $\underset{\sim}{\nabla} A_o$ is the beginning of the gauge invariant field strength tensor. Next, evaluating Fig. 5a + 5b using the rules of Appendix A, and restricting the emitted gluon to be of spacelike polarization yields two terms of different spin structure. The spin singlet term corresponds to the spacelike gluon coupling to the quark color convection current, and yields after manipulations similar to those used deriving Eq. 1.5

$$(5a + 5b, \text{ spacelike}) = -\frac{(2\pi)^3\delta^3(P_f - P_i)}{V^{3/2}(2k_o)^{1/2}} \frac{(igT_b)_{\alpha\beta}}{\sqrt{3}} \delta_{s_1 s_1'} \delta_{s_2 s_2'}$$

$$\times \sum_{n=0}^{\infty} <\phi|\frac{2p_Q^i}{m} \frac{1}{(H_8 + \varepsilon_1)^{n+1}}|Q\bar{Q}>_8 (\partial_o)^n A_i^b \quad . \tag{1.6}$$

Note that the sum of Eq. 1.5 and Eq. 1.6 does not give a gauge invariant result. The spin flip term corresponds to the spacelike gluon coupling to the quark spin current, and yields the independently

gauge invariant expression

$$(5a + 5b, \text{ spacelike}) = \frac{i(2\pi)^3\delta^3(P_f - P_i)}{V^{3/2}\,(2k_o)^{1/2}}\,\frac{(igT_b)_{\alpha\beta}}{\sqrt{3}}$$

$$\times \sum_{n=0}^{\infty}\Bigg\{\chi^+_{s_1'}\sigma_j\chi_{s_1}\,\delta_{s_2s_2'}\Big\langle\Phi\Big|\frac{1}{(H_8+\epsilon_1)^{n+1}}\Big|Q\bar{Q}\Big\rangle_8(\partial_o)^n\,\frac{[k\times A^b]^j}{2m}$$

$$+\ \delta_{s_1s_1'}\chi^+_{s_2'}\sigma_j\chi_{s_2}\Big\langle\Phi\Big|\frac{1}{(H_8+\epsilon_1)^{n+1}}\Big|Q\bar{Q}\Big\rangle_8(\partial_o)^n\,\frac{[k\times A^b]^j}{2m}\Bigg\} \tag{1.7}$$

where χ is the non-relativistic quark two-component spinor. In order to evaluate Fig. 5c, we first isolate the effective interaction induced by the three-gluon-vertex. This is done by calculating Fig. 6 in the limit of $(x - y) \to 0$. Also note that the legs which ultimately connect to quark lines have timelike polarization to lowest order in p/m_Q. Therefore, in Feynman gauge, with $\lambda = j$ = spacelike

$$(\text{Fig. 6}) = gt_{bac}A^j_b(x)\int d^4w(\partial^j_x - \partial^j_y)\,\frac{1}{4\pi^2(x-w)^2}\,\frac{1}{4\pi^2(y-w)^2}$$

which reduces to

$$(\text{Fig. 6}) = -\frac{gt_{bac}A^j_b(x)(y-x)_j}{4\pi^2(y-x)^2}\quad . \tag{1.8}$$

We can now make the insertion of Fig. 6 onto the quark lines which yields Fig. 5c. After manipulations similar to those used deriving Eq. 1.5, we find

$$(\text{Fig. 5c}) = \frac{i(2\pi)^3\delta^3(P_f - P_i)}{V^{3/2}\,(2k_o)^{1/2}}\,\frac{3g^2}{8\pi}\,\frac{(igT_b)_{\alpha\beta}}{\sqrt{3}}\,\delta_{s_1s_1'}\,\delta_{s_2s_2'}$$

$$\times \sum_{n=0}^{\infty}\Big\langle\Phi\Big|\frac{r_i}{r}\,\frac{1}{(H_8+\epsilon_1)^{n+1}}\Big|Q\bar{Q}\Big\rangle_8(\partial_o)^nA^i_b\quad . \tag{1.9}$$

However, this term can be written in a way which makes manifest the fact that it is effectively the same order in g^2 as the terms from Figs. 5a and 5b. This is done by using the relation $H_8 - H_1 = 3g^2/8\pi r$ which is derived in Appendix B and valid for QCD in Coulomb approximation, and the commutation relation $[H_8, r_i] = -2ip_i/m$, which yields

$$\text{(Fig. 5c)} = \frac{i(2\pi)^3\delta^3(P_f - P_i)}{V^{3/2}\,(2k_o)^{1/2}} \frac{(igT_b)_{\alpha\beta}}{\sqrt{3}} \delta_{s_1 s_1'} \delta_{s_2 s_2'}$$

$$\times \sum_{n=0}^{\infty} \left[< \phi | r_i \frac{1}{(H_8 + \epsilon_1)^n} |Q\bar{Q}>_8 (\partial_o)^n A_b^i \right. \qquad (1.10)$$

$$\left. + < \phi | - \frac{2ip_Q^i}{m} \frac{1}{(H_8 + \epsilon_1)^{n+1}} |Q\bar{Q}>_8 (\partial_o)^n A_i^b \right].$$

Note that the first n = 0 term in Eq. 1.10, which is a potentially gauge non-invariant contribution, is zero because of the specific process computed, i.e.

$$< \phi | \underset{\sim}{r} \cdot \underset{\sim}{A}^b | Q\bar{Q} >_8 \, d^3p_Q d^3p_{\bar{Q}} \, \delta^3(p_Q + p_{\bar{Q}}) \sim \int d^3r \phi(r) \underset{\sim}{r} \cdot \underset{\sim}{A}_b \delta^3(r) \sim 0$$

since $\phi(r)$ is finite as $r \to 0$. Now adding together Eq. 1.5, 1.6, and 1.10 yields for the non-spin-flip part of the sum of diagrams 5a, 5b, and 5c, the gauge invariant expression (to lowest order)

$$\text{(Fig. 5)} = -\frac{i(2\pi)^3\delta^3(P_f - P_i)}{V^{3/2}\,(2k_o)^{1/2}} \frac{(igT_b)_{\alpha\beta}}{\sqrt{3}} \delta_{s_1 s_1'} \delta_{s_2 s_2'} \qquad (1.11)$$

$$\times \sum_{n=0}^{\infty} < \phi | r_i \frac{1}{(H_8 + \epsilon_1)^{n+1}} |Q\bar{Q}>_8 [(\partial_o)^n (\partial^i A_b^o - \partial^o A_b^i)]$$

while Eq. 1.7 is the gauge invariant expression for the spin flip part. Now that we have the gauge invariant expressions for the

$(Q\bar{Q})_C \to \phi + g$ matrix elements, we can go back and evaluate the S-matrix elements of Eq. 1.3 for specific final state ϕ's. Note that Eq. 1.7 corresponds to a color magnetic dipole transition, and Eq. 1.11 corresponds to a color electric dipole transition.

In retrospect, it should be no surprise that the diagrams of Fig. 4 are the complete gauge invariant set. The reason is that we are coupling an external gluon to a bound state, as given by Fig. 7 for the one gluon exchange potential. If we connect the external gluon in all possible ways to the bound state, to lowest order we generate just the set of diagrams given by Fig. 4.

IV. Results for charmonium production

Using Eq. 1.7 and 1.11 we can now evaluate the S-matrix elements of Eq. 1.3. The possible quarkonia final states are the $\eta(^1S_o)$ and the $\chi(^3P_J)$. The Ψ state is not allowed due to charge conjugation invariance. For $\eta(^1S_o)$ production only the color magnetic dipole transition operator of Eq. 1.7 is of relevance due to the spin structure, i.e. $"g"(^3S_1) \to Q\bar{Q}(^3S_1) \to Q\bar{Q}(^1S_o) + g(^3S_1)$. Doing the spin = 0 projection, the sum over all n, and substituting $p_Q^2/m_Q + \varepsilon_B$ for H_B, the amplitude for $"g" \to \eta + g$ becomes

$$S\left[\eta(^1S_o)\right] = -\frac{i(2\pi)^4\delta^4(Q - P - k)g^2\underline{\varepsilon}^a\cdot(\underline{k}\times\underline{\varepsilon}_b)}{(2Q)^{1/2}\,(2k_o)^{1/2}\,V\,\sqrt{6}}\,\frac{d^3p_Q}{(2\pi)^3}$$

$$\times\ \langle {}^1S_o|\ \frac{1}{m(\varepsilon_T - k_o) + p_Q^2 - i\varepsilon}\ |\ Q\bar{Q}\rangle_B \qquad (1.12)$$

where $\underline{\varepsilon}^a$ and $\underline{\varepsilon}^b$ are the polarization vectors of the incident and final state gluons, and $\varepsilon_T = \varepsilon_1 + \varepsilon_B$. Note that the amplitude

has the expected physical behavior of developing a finite absorptive part when $k_o > \varepsilon_T$, i.e. when $Q > 2m_Q + \varepsilon_g$, which is the threshold for "physical" intermediate colored states. Using the coulombic 1S bound state wavefunction for the matrix element, squaring the amplitude and summing over final states, yields for the rate

$$R("g" \to \eta + g) = \frac{g^4(Q - m_\eta)^3}{36\pi^2 Q a^3 \left| \left[\frac{1}{a} + \sqrt{m(\varepsilon_T + m_\eta - Q)}\right]^2 \right|^2} \qquad (1.13)$$

where a is the Bohr radius. For $\chi(^3P_J)$ production, spin structure demands that only the color electric dipole transition operator of Eq. 1.11 contributes to the amplitude, i.e. $"g"(^3S_1) \to Q\bar{Q}(^3S_1) \to Q\bar{Q}(^3P_J) + g(^3S_1)$. We find the ^3P_J states produced with their statistical weight $R^{J=0}:R^{J=1}:R^{J=2}$ equal to 1:3:5 and

$$R\left("g" \to \chi(^3P_J) + g\right) = \frac{g^4(Q - m_\chi)^3 m^2(2J+1)}{432\pi^2 Q \left| \left[\sqrt{m(\varepsilon_T' + m_\chi - Q)} + \frac{1}{2a}\right]^2 \right|^4 a^5} \qquad (1.14)$$

where $\varepsilon_T' = \frac{1}{4}\varepsilon_1 + \varepsilon_g$ and m_χ is the χ-state mass.

To make the connection to the branching ratio of T to charmonium, one can make use of Fritzsch's results by dividing out the rate of $"g" \to c\bar{c}$ and multiplying by the rate of $"g" \to \Phi + g$, where Φ denotes either η_c or $\chi_c(^3P_J)$. These scaling factors which must be applied to the results of Fig. 2 are, for η_c production

$$\frac{R("g" \to \eta_c + g)}{R("g" \to c\bar{c})} = \frac{4g^2(Q - m_{\eta_c})^3}{9\pi a^3 \left| \left[1/a + \sqrt{m(\varepsilon_T + m_{\eta_c} - Q)}\right]^2 \right|^2 (Q^2 - m_{\eta_c}^2)^{1/2} Q} \qquad (1.15)$$

and for χ production

$$\frac{R("g" \to \chi_c + g)}{R("g" \to c\bar{c})} = \frac{g^2 m^2 (Q - m_{\chi_c})^3}{3\pi a^5 Q \left|\left[\frac{1}{2a} + \sqrt{m(\epsilon_T' + m_{\chi_c} - Q)}\right]^2\right|^4 (Q^2 - m_{\eta_c}^2)^{1/2}} \quad . \tag{1.16}$$

To apply these results to the charmonium system, the values of the bound state parameters can be determined from fitting m_ψ and $m_{\psi'}$ to a color coulomb spectrum (one gluon exchange potential). We find $m_c = 1.9$ GeV and $a = .81$ GeV^{-1}. The numberical evaluation of Eq. 1.15 and Eq. 1.16 is found in Tables 1 and 2. They need only be evaluated up to an incident energy of 3.75 GeV, as above this, $D\bar{D}$ production dominates.

If our "scaling factors" in Tables 1 and 2 are folded with the Fritzsch results of Fig. 2, one obtains for the branching ratio of T to η_c + anything

$$BR(T \to \eta_c + X) \approx 3 \times 10^{-5} \tag{1.17}$$

and for T to χ_c + anything

$$BR(T \to \chi_c + X) \approx 3 \times 10^{-6} \quad . \tag{1.18}$$

Note that this branching ratio is between 10^{-2} and 10^{-3} times smaller than that predicted using the assumption of duality, and the associated implicit assumption of dynamical resonance enhancement. (A branching ratio of 10^{-2} to ψ states would just be observable in current CESR experiments [5]). Thus, the lack of colored resonances allows heavy quarkonium production with soft gluon emission to be suppressed by limited phase space and the small multipole type coupling.

Next, we must critically analyze the approximations used in this calculation.

V. Analysis of approximation

Any calculation of a quantity to be compared with experiment must have means available to estimate neglected contributions to the process under consideration. We will, in order, discuss the corrections due to higher order gluon emission, higher order terms in the multipole expansion, relativistic corrections, and the validity of the one gluon exchange potential for the charmonium binding.

A. Higher order gluon emission

In addition to the lowest order diagram where one gluon is emitted to effect color neutralization, there can be two soft gluons emitted from the $Q\bar{Q}$ state. Adding a second gluon emission to the lowest order term results in Fig. 8. Using the form of the color El operator for $g - Q\bar{Q}$ coupling given in Eq. 1.11, this contribution can be crudely estimated.

$$(\text{correction}) \sim \left[\frac{g(k_2^o a)}{\sqrt{2k_2^o}} \frac{1}{(H_8 + \varepsilon_1 - k_2^o)} \right]^2 \frac{d^3k_2}{(2\pi)^3}$$

$$\sim \frac{g^2 (k_2^o a)^2}{\left[\left\langle \frac{p_Q^2}{m_Q} \right\rangle \right]^2} \frac{d^3k_2}{2k_2^o (2\pi)^3}$$

$$\sim \frac{\alpha_s}{\pi} (k_2^o a)^2 \left(\frac{k_2}{\varepsilon} \right)^2$$

For $|k_1| \sim |k_2| \sim$ (available kinetic energy)/2 $\sim$ .35 GeV, $a \sim .81\ \text{GeV}^{-1}$, and $\varepsilon \sim .8$ GeV, we find

(correction) $\sim 10^{-3}$.

This is much less than one, and indicates that higher order gluon emission does not contribute significantly. Also note that this is essentially equivalent to a "back-of-the-envelope" calculation of the suppression factor induced by the lowest order term.

B. Neglected terms in the multipole expansion

Our restriction to the lowest order multipole occurred during the following typical approximation

$$[A_o^b(R + \tfrac{r}{2}) - A_o^b(R - \tfrac{r}{2})] \approx \underset{\sim}{r}\cdot\underset{\sim}{\partial} A_o^b(R) + \frac{2}{3!}\left(\frac{\underset{\sim}{r}\cdot\underset{\sim}{\partial}}{2}\right)\left(\frac{\underset{\sim}{r}\cdot\underset{\sim}{\partial}}{2}\right)\left(\frac{\underset{\sim}{r}\cdot\underset{\sim}{\partial}}{2}\right) A_o^b(R) + \ldots$$

when only the first term in the expansion was retained. We expect that when higher order terms are kept, we generate the full gauge invariant expression

$$\text{(multipole expansion)} \sim \underset{\sim}{r}\cdot\underset{\sim}{E}^a + \frac{1}{3}\frac{r^i}{2}\frac{r^j}{2}\frac{r^k}{2} D_i D_j E_k^a + \ldots$$

where D_i is the covariant derivative. Then, in the amplitude, very crudely,

$$\text{(lowest order)} \rightarrow \text{(lowest order)} \left(1 + \frac{(ak_o)^2}{24}\right) .$$

In the rate, this is less than a 5% correction.

C. Relativistic corrections

The non-relativistic Feynman rules used the following typical approximation

$$\bar{U} \gamma_o U \xrightarrow{\text{N.R.}} \chi^+ \chi + O\left(\frac{p^2}{4m_Q^2}\right) .$$

using $P^2/m_Q \sim \epsilon \sim .8$ GeV gives $P^2/4m_Q^2 \sim 0.1$. This means that relativistic corrections could be as large as 20% in the calculated rates. This is not completely surprising since it is well known that the charmonium system has $\beta^2 \lesssim .3$, which is relatively large [6].

D. Validity of the one gluon exchange potential

It has been shown that non-perturbative effects dominate the perturbative 1/R one gluon exchange potential for charmonium systems [7]. Thus, as expected, the color coulomb potential does not reproduce the observed charmonium spectrum. However, for the following reason, it is a good model potential for this calculation.

The physical reason for the large suppression of Fritzsch and Streng's result is that the intermediate color octet $(Q\bar{Q})_8$ state in the process "g" $\rightarrow (Q\bar{Q})_8 \rightarrow$ "g" is always held off-shell. This is because the one gluon exchange potential in the color octet channel is repulsive, and raises the threshold for "physical" $(Q\bar{Q})_8$ production above the threshold for $D\bar{D}$ production. Therefore, the intermediate state is made virtual, and one never finds a dynamical enhancement due to colored resonances. Since colored resonances have not been observed out to very high energies, this is exactly the physical behavior that our amplitude should exhibit. In fact, if this calculation were done with the actual $V(Q\bar{Q})$ potential, we might expect an even greater suppression than observed here. This is because the experimental lower bounds on color octet state masses would require the intermediate state to be even more virtual than that given by the one gluon exchange potential. For this reason we believe our self-consistent calculation using the color

coulomb potential gives a reasonable order of magnitude estimate of the physical suppression mechanism.

Appendix

A. Non-relativistic Feynman rules

$$\bar{u}^{s'}(p')\gamma_o u^s(p) = \frac{1}{V}\left(\chi_{s'}^+, \chi_{s'}^+, \frac{\sigma\cdot p'}{E'+m}\right)\begin{pmatrix}\chi_s \\ \frac{\sigma\cdot p}{E+m}\chi_s\end{pmatrix}$$

$$= \frac{1}{V}\chi_{s'}^+\left(1 + \frac{\sigma\cdot p'\ \sigma\cdot p}{(E'+m)(E+m)}\right)\chi_s$$

$$\longrightarrow \frac{1}{V}\chi_{s'}^+\chi_s + 0\left(\frac{p^2}{4M^2}\right) \quad .$$

Similarly,

$$\bar{u}^{s'}(p')\gamma_k u^s(p) \longrightarrow \frac{1}{V}\chi_{s'}^+\left(\frac{(p+p')_k}{2m} + \frac{i\sigma\cdot[(p'-p)\times n_k]}{2m}\right)\chi_s \quad .$$

$$\bar{v}^s(p)\gamma^o v^{s'}(p) \longrightarrow \frac{1}{V}\chi_s^+\chi_{s'}^+ \quad .$$

$$\bar{v}^s(p)\gamma_k v^{s'}(p') \longrightarrow \frac{1}{V}\chi_s^+\left[\frac{(p+p')_k}{2m} + \frac{i\sigma\cdot[(p-p')\times n_k]}{2m}\right]\chi_{s'},$$

$$\bar{u}^{s'}(p')\gamma_o v^s(p) \longrightarrow \frac{1}{V}\chi_{s'}^+\left[\frac{\sigma\cdot p'}{2m} + \frac{\sigma\cdot p}{2m}\right]\chi_s$$

$$\bar{u}^{s'}(p')\gamma_k v^s(p) \longrightarrow \frac{1}{V}\chi_{s'}^+\sigma_k\chi_s$$

B. One Gluon exchange potential

$$H_8 - H_1 = \left(\frac{p_Q^2}{m} + V_8(r)\right) - \left(\frac{p_Q^2}{m} + V_1(r)\right)$$

$$= V_8(r) - V_1(r)$$

To calculate the one gluon exchange potential, we must evaluate the diagrams of Fig. 9.

$$V_8(r) - V_1(r) = -\frac{g^2}{4}\,\mathrm{Tr}(T^a T^b T^a T^b)\int_{-\infty}^{\infty}\frac{dt}{4\pi^2(r^2+t^2)}$$

$$+\frac{g^2}{3}\,\mathrm{Tr}(T^b T^b)\int_{-\infty}^{\infty}\frac{dt}{4\pi^2(r^2+t^2)}$$

$$= \frac{g^2}{24\pi r} + \frac{g^2}{3\pi r}$$

$$= \frac{3g^2}{8\pi r}$$

Note that the color singlet potential is attractive, and the color octet potential is repulsive.

References

1. H. Fritzsch and K.-H. Streng, Phys. Lett. 77B (1978) 299.
2. E. Poggio H. Quinn, and S. Weinberg, Phys. Rev. D13 (1976) 1958; H. Fritzsch and H. Leutwyler, Phys. Rev. D10 (1974) 1624.
3. Curt A. Flory, Phys. Lett. 94B (1980) 221.
4. M.E. Peskin, Nucl. Phys. B156 (1979) 365; G. Bhanot and M.E. Peskin, Nucl. Phys. B156 (1979) 391.
5. Kirk Shinsky, private communication.
6. H. Krammer and H. Krasemann, DESY report, DESY 79/20 (1979).
7. Curt A. Flory, LBL report LBL-11343, to appear in Phys. Lett. B.

Figure Captions

Fig. 1 T decay into charm + anticharm + hadrons

Fig. 2 Branching ratio of T to charm + anticharm as a function of $\xi = Q^2/m_T^2$, where Q^2 is the invariant mass squared of the $c\bar{c}$ pair.

Fig. 3 The modification made to the differential branching ratio due to including color neutralization of the $c\bar{c}$ pair.

Fig. 4 Gauge invariant set of diagrams for "g" → quarkonium + g. Q, k, and P are external four-momenta.

Fig. 5 Lowest order gluon emission from $Q\bar{Q}$ system. α, β, α', β', b are color indices and s_1, s_1', s_2, s_2' are spin states.

Fig. 6 Tri-gluon insertion in coordinate space. ω, x, y, z are coordinates, a, b, c are color indices, and λ, μ, ν are polarization indices.

Fig. 7 $Q\bar{Q}$ bound state where the potential is one-gluon-exchange.

Fig. 8 Emission of two gluons in the color neutralization of the

color octet $Q\bar{Q}$ pair. k_1 and k_2 are the gluon momenta.

Fig. 9 One gluon exchange potential for color octet and color singlet cases. a, b, c, and d are quark color indices, and T^m are the generators of $SU_c(3)$.

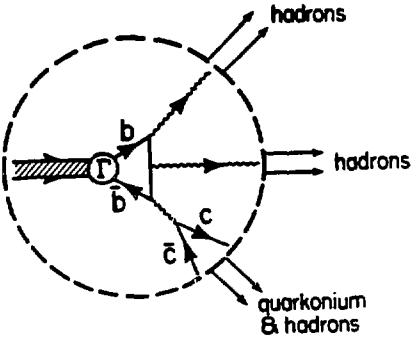
hadrons
b
Γ
b̄
hadrons
c
c̄
quarkonium
& hadrons

FIG. 1

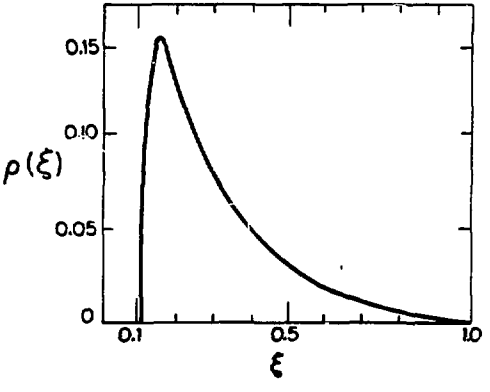
0.15
0.10
ρ(ξ)
0.05
0
0.1
0.5
1.0
ξ

FIG. 2

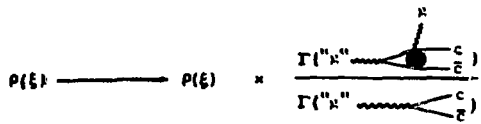

FIG. 3

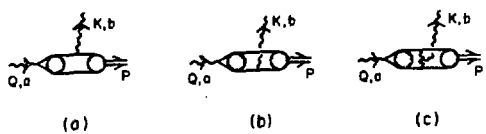

FIG. 4

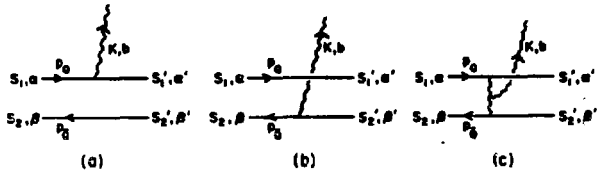

FIG. 5

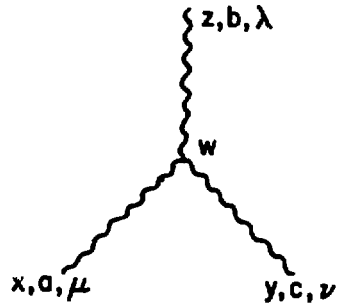

FIG. 6

FIG. 7

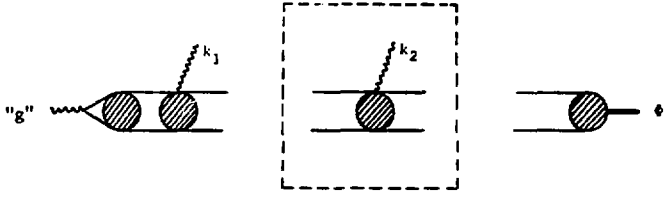

FIG. 8

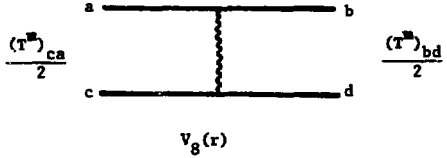
a
b
$\frac{(T^m)_{ca}}{2}$
$\frac{(T^m)_{bd}}{2}$
c
d
$V_8(r)$

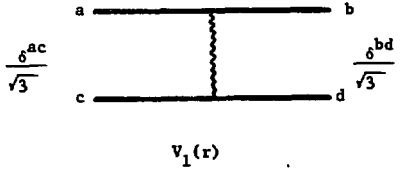
a
b
$\frac{\delta^{ac}}{\sqrt{3}}$
$\frac{\delta^{bd}}{\sqrt{3}}$
c
d
$V_1(r)$

FIG. 9

Table I

Q(in GeV)	$R_{\eta_c}/R_{c\bar{c}}$
3.0	0
3.1	3.7×10^{-5}
3.2	2.3×10^{-4}
3.3	7.1×10^{-4}
3.4	1.7×10^{-3}
3.5	3.4×10^{-3}
3.6	6.5×10^{-3}
3.7	1.2×10^{-2}
3.8	2.6×10^{-2}

Table II

Q(in GeV)	$R_X/R_{c\bar{c}}$
3.5	0
3.6	1.3×10^{-4}
3.7	2.3×10^{-3}
3.8	2.5×10^{-2}

CHAPTER II

F Meson Production in e^+e^- Annihilation

Abstract

The F meson production rate is calculated on the $\Psi(4414)$ resonance using non-relativistic multipole expansion techniques. The results indicate that this production mechanism could account for all or part of the observed rates.

I. Introduction

The charm model which successfully describes the properties of the established Ψ and D mesons, requires the existence of mesons having both charm and strangeness. These new particles, called F mesons, have the quantum numbers of a charmed quark and a strange antiquark. The only evidence which supports the presence of the F meson in e^+e^- annihilation has been presented by DASP [1]. Data from Mark II places an upper limit for F-production which is close to but less than the positive result of DASP [2]. It is now important to determine the production levels expected from theoretical considerations.

As before, we hope to be able to use non-relativistic approximations and a multipole expansion for coupling the gluonic degrees of freedom to the quark systems. This seems somewhat risky since strange quarks are involved, which only have a constituent mass on the order of 500 MeV. However by limiting ourselves to a kinematic regime only slightly above production threshold, it will be shown that the non-relativistic approximation is in fact reasonable, and the multipole expansion well behaved.

The process considered is the production of F mesons from a virtual photon produced in e^+e^- annihilation. As stated above, this demands a four quark final state consisting of charm + anticharm + strange + antistrange quarks. Figure 1 illustrates the production process where the incident virtual photon produces a color singlet $c\bar{c}$ pair which ultimately couples to an effectively local gauge invariant gluon operator, which is the source of the

strange quark content of the final state F mesons. Although the intermediate gluons are highly virtual and timelike, due to the limited phase space available they have a small three-momentum component. This long wavelength probe coupled to the small $c\bar{c}$ system naturally lends itself to a multipole expansion. The expansion parameter is of order $(\alpha_s \underset{\sim}{r}\cdot\underset{\sim}{k})$, where $\underset{\sim}{r}$ is the radius of the intermediate $c\bar{c}$ system and $\underset{\sim}{k}$ is the three-momentum of the intermediate gluon (which translates into the three-momentum of the produced final state strange quarks). As will be shown, the relatively small value of this quantity affords good justification for our lowest order calculation.

II. The four-quark production amplitude

The first step of the calculation is to evaluate the four-quark production amplitude of Fig. 1, which must later be projected onto the desired $F\bar{F}$ state. The four-quark production amplitude can be split into two parts for computational ease. We will first focus exclusively upon the charmed quark production and its coupling to the intermediate gluon modes as given by Fig. 2, and later attach the final state strange quarks. Note that only one time ordering is relevant for this part of the process since the produced charmed quarks are very massive and only slightly off shell. This part of the amplitude is given by

$$\begin{aligned} A(\text{"}\gamma\text{"} \to Q_c\bar{Q}_c + X) \;=\; & -ieQ_c(2\pi)\delta(E_f - E_i) \\ & \times \langle X Q_c\bar{Q}_c | \int_0^\infty dt H_I(t) e^{-iHt} | Q_c'\bar{Q}_c' \rangle \qquad (2.1) \\ & \times \langle Q_c'\bar{Q}_c' | H_{EM}(0) | \text{"}\gamma\text{"} \rangle \frac{d^3p_c'}{(2\pi)^3} \frac{d^3\bar{p}_c'}{(2\pi)^3} \end{aligned}$$

where $H_I(t)$ is the operator which couples the charmed quarks to the intermediate gluon state, which is denoted by X. The evaluation of the first matrix element in Eq. 2.1 uses the now familiar techniques for coupling gluons of small three-momentum to heavy non-relativistic quark bound states [3]. To obtain the complete gauge invariant local gluon operator (including the non-abelian term that was neglected for kinematic reasons in Chapter I), it is necessary to sum all the diagrams of Fig. 3. In order to get the explicit form and normalization of this operator, one must temporarily model the quark-antiquark interaction as being mediated by "color-coulomb" ladder exchange. Once the gauge invariant operator is obtained, it can be used to couple external gluons to a quark bound state whose internal binding mechanism deviates from a simple coulomb-like potential. (This is shown in the approach by Yan [3], which does not rely on the form of the $Q\bar{Q}$ potential for the derivation of the multipole expansion.) The reduction of the matrix element yields

$$\begin{aligned} \langle X Q_c \bar{Q}_c | \int_0^\infty dt H_I(t) e^{-iHt} | Q_c' \bar{Q}_c' \rangle &= (2\pi)^3 \delta^3(p_f - p_i)(igT_b)_{\alpha\bar{\alpha}} \delta_{\lambda_c \lambda_c'} \delta_{\bar{\lambda}_c \bar{\lambda}_c'} \\ &\times \langle X Q_c \bar{Q}_c | r_i \frac{1}{\frac{p_c'^2}{m_c} + \varepsilon' - \varepsilon - (p_s^o + \bar{p}_s^o)} | Q_c' \bar{Q}_c' \rangle \\ &\times (\partial^i A_b^o - \partial^o A_b^i - g f_{bac} A_a^o A_c^i) \end{aligned} \tag{2.7}$$

where $\varepsilon'(\varepsilon)$ is the interaction potential energy of the $c\bar{c}$ pair in the color singlet (octet) state, r_i is the relative separation of the $c\bar{c}$ pair, and $(p_s^o + \bar{p}_s^o)$ is the energy of the emitted gluonic system.

Note that this is simply the non-abelian analogue of the electric dipole ($\underset{\sim}{r}\cdot\underset{\sim}{E}$) transition familiar from electromagnetism. It is easy to show that the magnetic dipole coupling does not contribute to this order in the non-relativistic expansion.

To calculate the contribution from intermediate $c\bar{c}$ resonances we note that the energy denominator that appears in Eq. 2.2 is exactly $(m_{res} - Q)$, where Q is the center of mass energy, and m_{res} is the mass of the relevant resonance, i.e.

$$\frac{p_c'^2}{m_c} + \varepsilon' - \varepsilon - p_s^o - \bar{p}_s^o = \frac{p_c'^2}{m_c} + \varepsilon' - \varepsilon - p_s^o - \bar{p}_s^o + 2m_c - 2m_c$$

$$= (2m_c + \varepsilon' + \frac{p_c'^2}{m_c}) - (2m_c + p_2^o + \bar{p}_2^o + \varepsilon)$$

$$= m_{res} - Q \ .$$

To complete the evaluation of Eq. 2.2, we note that the expectation value of r_i for the $\ell = 0$ bound state to free quark transition can be estimated without knowing the exact bound state wavefunction:

$$r_i \approx v_i^{rel} \times \begin{pmatrix} \text{bound state} \\ \text{coherence time} \end{pmatrix} \approx \left(\frac{2p_c'}{m_c}\right)_i \times \frac{1}{E} \qquad (2.3)$$

where $E = |m_{res} - 2m_c|$. This relationship holds exactly for a coulombic bound state, and is a good approximation for a harmonic oscillator potential.

We can now trivially couple the gluon fields of Eq. 2.2 to an $s\bar{s}$ pair as in Fig. 1 and obtain the amplitude to lowest order in the three momentum:

$$A("\gamma" \to Q_c\bar{Q}_c Q_s\bar{Q}_s) = \frac{(ieQ_c)(igT_b)_{\alpha\bar{\alpha}}(igT_b)_{\beta\bar{\beta}}}{2m_s}(\chi^+_{\lambda_s}\sigma_i\chi_{\lambda_{\bar{s}}})(\chi^+_{\lambda_c}\sigma_\mu\chi_{\lambda_{\bar{c}}})$$

$$\times \frac{2p_c'^i}{m_c E}\frac{(1-\frac{3\alpha_s}{4})}{(Q - m_{res} - i\Gamma_{res}/2)}(2\pi)^4\delta^4(P_f - P_i) \qquad (2.4)$$

where μ is the virtual photon's Lorentz index, and the χ's are non-relativistic quark two-spinors. The appearance of the factor $(1 - \frac{3\alpha_s}{4})$ is from the sum of the tree diagram of Fig. 1a and the one loop diagram of Fig. 1b [4]. This four-quark production amplitude can now be projected onto the desired color singlet final states to determine the $F\bar{F}$ production amplitude.

III. F meson production

To obtain the $F\bar{F}$ final states from the four-quark production amplitude of Eq. 2.4, we must do color, spin, and momentum wavefunction projections. We define the center-of-mass momentum and internal momentum of the F meson to be $\underset{\sim}{P} \equiv \underset{\sim}{p}_c + \underset{\sim}{\bar{p}}_s$ and $\underset{\sim}{q} \equiv \underset{\sim}{p}_c - \underset{\sim}{\bar{p}}_s$, and of the $\bar{F}$ by $\underset{\sim}{\bar{P}} \equiv \underset{\sim}{\bar{p}}_c + \underset{\sim}{p}_s$ and $\underset{\sim}{\bar{q}} \equiv \underset{\sim}{\bar{p}}_c - \underset{\sim}{p}_s$. The momentum wavefunction projection becomes

$$A\left("\gamma" \to (Q_c\bar{Q}_s)(\bar{Q}_c Q_s)\right) = A("\gamma" \to Q_c\bar{Q}_c Q_s\bar{Q}_s) \times \frac{d^3q}{(2\pi)^3}\Phi_F(q)$$

$$\times \frac{d^3\bar{q}}{(2\pi)^3}\Phi_{\bar{F}}(\bar{q})$$

$$= A("\gamma" \to Q_c\bar{Q}_c Q_s\bar{Q}_s) \times \Psi_F(0) \times \Psi_{\bar{F}}(0) \qquad (2.5)$$

where $\Phi_F(\Psi_F)$ is the momentum (spatial) wavefunction of the F meson,

and all terms linear in $\underset{\sim}{q}$ and $\bar{\underset{\sim}{q}}$ integrate to zero due to the $\ell = 0$ nature of the F. The color projection operator to be inserted in Eq. 2.4 is simply $\delta_{\alpha\bar{\beta}}\delta_{\bar{\alpha}\beta}/3$. The spin projections are equally simple. Define

$$R_{i\mu} \equiv (\chi^{+}_{\lambda_s}\sigma_i\chi_{\bar{\lambda}_s})(\chi^{+}_{\lambda_c}\sigma_\mu\chi_{\bar{\lambda}_c}) \quad . \tag{2.6a}$$

In appendix A, it is shown that for $F\bar{F}$ production

$$R^{F\bar{F}}_{i\mu} = \delta_{i\mu} \quad , \tag{2.6b}$$

for $F^*\bar{F}$ production

$$R^{F^*\bar{F}}_{i\mu} = -i\sqrt{2}\,\varepsilon_{i\mu j}\epsilon^{j}_{\lambda} \tag{2.6c}$$

with $\underset{\sim}{\epsilon}_\lambda$ being the F^* polarization vector, and for $F^*\bar{F}^*$ production

$$R^{F^*\bar{F}^*}_{i\mu} = 2(\varepsilon^{\bar{\lambda}}_i\epsilon^{\lambda}_\mu - \underset{\sim}{\varepsilon}^{\bar{\lambda}}\cdot\underset{\sim}{\epsilon}^{\lambda}\delta_{i\mu} + \varepsilon^{\lambda}_i\epsilon^{\bar{\lambda}}_\mu) \tag{2.6d}$$

with $\underset{\sim}{\epsilon}^{\lambda}$ and $\underset{\sim}{\varepsilon}^{\bar{\lambda}}$ the polarization vectors for the F^* and $\bar{F}^*$ respectively. The projected amplitude becomes

$$A\left("\gamma" \to (Q_c\bar{Q}_s) + (\bar{Q}_cQ_s)\right) = \frac{-2ig^2eQ_c\psi_F(0)\psi_{\bar{F}}(0)R_{i\mu}(1-\frac{3\alpha_s}{4})P^i(2\pi)^4\delta^4(P_f - P_i)}{3m_cm_sE(Q - m_{res} - i\Gamma_{res}/2)} \quad . \tag{2.7}$$

Adding on the $(e^+e^- \to "\gamma")$ part of the amplitude, squaring, and summing over final states yields

$$\sigma(F\bar{F}\text{ - production}) = \frac{(4\pi\alpha_s)^2(4\pi\alpha Q_c)^2|\psi_F(0)|^2|\psi_{\bar{F}}(0)|^2(1-\frac{3\alpha_s}{4})^2m_F^{5/2}(Q - m_F - m_{\bar{F}})^{3/2}R}{27\pi m_c^2m_s^2E^2\left[(Q - m_{res})^2 + \Gamma^2/4\right]Q^4} \tag{2.8}$$

where R is the statistical spin factor, and is equal to (1, 4, 7) for ($F\bar{F}$, $F^*\bar{F} + F\bar{F}^*$, $F^*\bar{F}^*$) production. An interesting feature of this calculation is that the quark binding interaction has not entered in any complicated way. The binding interaction only entered through the F meson wavefunction at the origin, which can be estimated from an experimentally determined equation [5] using only the constituent quark masses.

The production cross section for $F\bar{F}$ states can now be evaluated as a function of energy using Eq. 2.8. We use the DASP values $m_F = 2.03$ GeV and $m_{F^*} = 2.14$ GeV for the F meson masses. The constituent charm and strange quark masses are 1.5 GeV and 0.5 GeV respectively. Using these quark masses one estimates [5] $|\psi_F(0)|^2 = 1.1 \times 10^{-2}$ GeV^3, and α_s is defined at the mass scale of the bound state to which it is associated. Finally, we can now evaluate the $F\bar{F}$ production cross section contribution from the narrow ($c\bar{c}$) resonance at 4.414 GeV, whose measured width is 33 ± 10 MeV [6]. We find for all possible F meson spin states

$$\sigma_{F\bar{F}}(Q = 4.4 \text{ GeV}) = 1.4 \text{ nb}^{+1.4 \text{ nb}}_{-\ .6 \text{ nb}} \tag{2.9}$$

where the limits are from the experimental uncertainty in the resonance width. This contribution to $F\bar{F}$ production is very strongly peaked in energy and drops to less than 5% of its peak value as one tunes the energy more than 100 MeV off resonance. The spin state content of this cross section is in the multiple ratio

$$F\bar{F}:F^*\bar{F} + F\bar{F}^*:F^*\bar{F}^* = 1:2.2:1.4 \tag{2.10}$$

The experimental cross sections, after taking estimated branching

ratios into account are, from DASP's inclusive η-production data [1]

$$\sigma_{F\bar{F}}(Q = 4.4\ \text{GeV}) = 5.3\ \text{nb}^{+1.3}_{-1.2}\ \text{nb} ,$$

and for Mark II from ηπ production, the obtained upper limit [2]

$$\sigma_{F\bar{F}}(Q = 4.4\ \text{GeV}) < 3\ \text{nb} .$$

Thus our calculated F meson production mechanism could account for all or most of the observed rate.

IV. Validity of approximations

We will discuss, in order, the validity of the perturbative multipole expansion, the non-relativistic reduction of the four-component quark spinors, and the neglect of possible perturbative final state interactions.

A. The perturbative multipole expansion

The multipole expansion parameter is, very crudely $\alpha_s(\underset{\sim}{r}\cdot\underset{\sim}{k})$. Using Eq. 2.3 for $\underset{\sim}{r}$

$$\alpha_s(\underset{\sim}{r}\cdot\underset{\sim}{k}) \longrightarrow \alpha_s(r)(k)$$
$$\sim \alpha_s(\tfrac{1}{\epsilon}\beta)(P)$$

where ϵ is the $Q\bar{Q}$ interaction energy ($\sim m_{res} - 2m_c$), β is the relative $Q\bar{Q}$ velocity in the resonance, and P is the final state three-momentum. Defining α_s at the scale of the ψ-resonance gives

$$\alpha_s(\underset{\sim}{r}\cdot\underset{\sim}{k}) \sim .15$$

for $F\bar{F}$ production at a center of mass energy of 4.4 GeV. Thus, the multipole expansion parameter seems under control.

B. Relativistic corrections

The weakest possible link in the use of the non-relativistic Feynman rules is the reduction of the production vertex of the $\bar{s}s$ pair:

$$\bar{u}(p_s)\gamma_i v(\bar{p}_s) \longrightarrow \chi_s^+ \sigma_i \chi_{\bar{s}} + O\left(\frac{p\cdot\bar{p}}{(\quad + m)^2}\right)$$

$$\sim \left(1 + \frac{(P/2)^2}{(2m_s)^2}\right)$$

$$\sim (1 + .13) \quad .$$

This means that there could be relatively large relativistic corrections to our calculated rates on the order of 25%.

C. Perturbative final state interactions

There exist possible final state interactions as in Fig. 4. Figure 4a is already implicitly included through the use of the effective coupling constant in the lowest order diagram. The color trace of Fig. 4b is down by $1/N_c$ from the lowest order diagram, indicating that the expansion parameter here is in fact α_s/N_c, as expected from meson-meson scattering in the $1/N_c$ expansion [7]. So even for an $\alpha_s \sim .3 - .4$, neglect of these terms seems reasonable.

As we can see from A, B, and C above, the approximations used in the calculation of F meson production seem to be under control. The most important test remaining is an independent reproduction of the DASP results.

Appendix

A. Spin projections

$$R_{i\mu} \equiv (\chi^{+}_{s_2}\sigma_i\chi^{-}_{s_2})(\chi^{+}_{s_1}\sigma_\mu\chi^{-}_{s_1})$$

The normalized spin-1 vectors are

$$\underset{\sim}{\varepsilon}^{+} = -\frac{1}{2}(1, -i, 0)$$

$$\underset{\sim}{\varepsilon}^{-} = \frac{1}{2}(1, i, 0)$$

$$\underset{\sim}{\varepsilon}^{o} = \frac{1}{\sqrt{2}}(0, 0, 1) \quad .$$

For $F\bar{F}$ production

$$R_{i\mu} = \left(\frac{1}{\sqrt{2}}\right)^2 \mathrm{Tr}(\sigma_i\sigma_\mu) = \delta_{i\mu} \quad .$$

For $F^*\bar{F}$ production

$$R_{i\mu} = \frac{1}{\sqrt{2}}\mathrm{Tr}\,(\sigma_i\underset{\sim}{\varepsilon}^{\lambda}\cdot\underset{\sim}{\sigma}\sigma_\mu) = -i\sqrt{2}\,\varepsilon_{i\mu j}\,\varepsilon^{j}_{\lambda} \quad .$$

For $F^*\bar{F}^*$ production

$$R_{i\mu} = \mathrm{Tr}(\underset{\sim}{\varepsilon}^{\bar{\lambda}}\cdot\underset{\sim}{\sigma}\,\sigma_i\,\underset{\sim}{\varepsilon}^{\lambda}\cdot\underset{\sim}{\sigma}\,\sigma_\mu)$$

$$= 2(\varepsilon^{\bar{\lambda}}_{i}\varepsilon^{\lambda}_{\mu} - \underset{\sim}{\varepsilon}^{\lambda}\cdot\underset{\sim}{\varepsilon}^{\bar{\lambda}}\,\delta_{i\mu} + \varepsilon^{\lambda}_{\mu}\varepsilon^{\bar{\lambda}}_{i}) \quad .$$

References and Footnotes

1. DASP collaboration, R. Brandelik et.al., Phys. Lett. 80B (1979) 412.
2. V. Lüth, Invited talk given at the 1979 International Symposium on Lepton and Photon Interactions at High Energies, Batavia, IL, August 1979.
3. M.E. Peskin, Nucl. Phys. B156 (1979) 365; K. Shizuya, LBL Report No. LBL-11004 (to be published); T.-M. Yan, Phys. Rev. D22 (1980) 1652.
4. MAXYMA was used to do the Feynman parameter integral of Fig. 1b.
5. J.D. Jackson, Proceedings of the SLAC Summer Institute on Particle Physics, Stanford, CA, August 1976.
6. J. Siegrist et. al., Phys. Rev. Lett. 36 (1976) 700.
7. S. Coleman, Proceedings of the International School of Subnuclear Physics, Erice, Italy, July 1979.

Figure Captions

Fig. 1 "γ" $\to Q_c\bar{Q}_c Q_s\bar{Q}_s$ diagrams. λ is the quark spin index, α and β are color indices.

Fig. 2 The gluon/$(c\bar{c})$ resonance coupling.

Fig. 3 Gauge invariant set of diagrams that gives the local gluon operator which couples to the $c\bar{c}$ resonance.

Fig. 4 Possible final state corrections to calculated production mechanism.

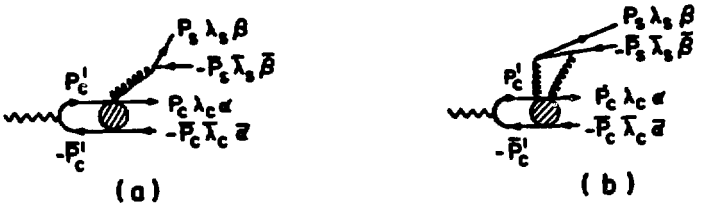
$P_s \lambda_s \beta$
$-\bar{P}_s \bar{\lambda}_s \bar{\beta}$
P_c'
$P_c \lambda_c \alpha$
$-\bar{P}_c \bar{\lambda}_c \bar{\alpha}$
$-\bar{P}_c'$
(a)
$P_s \lambda_s \beta$
$-\bar{P}_s \bar{\lambda}_s \bar{\beta}$
P_c'
$P_c \lambda_c \alpha$
$-\bar{P}_c \bar{\lambda}_c \bar{\alpha}$
$-\bar{P}_c'$
(b)

FIG. 1

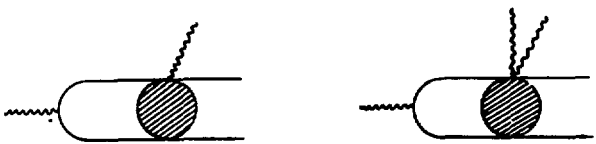

FIG. 2

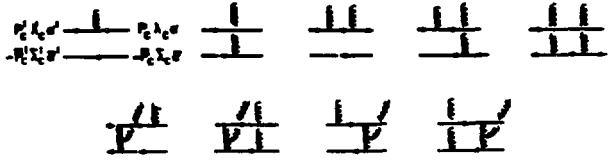

FIG. 3

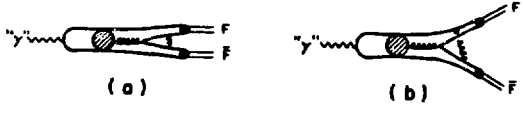

FIG. 4

CHAPTER III

Non-perturbative Effects in Heavy Quarkonia

Abstract

The effect of a non-zero vacuum gluon condensate on heavy quarkonia is discussed. As a function of the quark mass, it is determined which low lying levels of the spectrum are dominated by the perturbative 1/R one gluon ladder exchange potential.

I. Introduction

In QCD, due to asymptotic freedom, it is well known that the short distance part of the potential is dominated by one gluon exchange, giving rise to a calculable 1/R potential. For the long distance part of the interaction, various phenomenological potentials have been postulated that reproduce the observed heavy hadronic spectrum. Since the bound state quarkonium radius dimensionally goes like $r \sim \frac{1}{m_Q}$, one of the hopes is that for very heavy quarks the bound state radius will be of a size that only samples the known short distance part of the potential, allowing unambiguous theoretical calculations. A crude back-of-the-envelope estimate of how massive the quarks must be to see only the "color coulomb interaction" is made by requiring that the coulomb-like binding energy is much greater than some hadronic energy scale

$$\left[\frac{4}{3}\alpha_s\right]^2 \frac{m_Q}{4n^2} > 1 \text{ GeV} \tag{3.1}$$

where n is the principal quantum number of the coulomb bound state. Choosing the strong interaction scale parameter λ to be approximately 500 MeV, and the effective coupling constant to be at the scale of the bound state Bohr radius yields $m_Q > 25$ GeV for $n = 1$.

It is now possible to determine more rigorously which low lying levels of the heavy quark bound state spectrum are dominantly coulombic, as a function of the quark mass. The procedure will be to calculate the non-perturbative power corrections to the 1/R potential for extremely large quark masses where these power corrections are known to be small, and then determine how small the

quark masses can become before the coulomb approximation breaks down. The method for studying these non-perturbative effects is due to the pioneering work of Shifman, Vainshtein, and Zakharov [1]. Their technique is to extract the long distance behavior of internal lines in Feynman diagrams systematically, and parameterize this dynamical contribution with experimentally determined quantities (see Appendix A). As applied to a heavy quark-antiquark bound state, the procedure is to take the lowest order perturbative diagrams of Fig. 1 for gluon exchange within the $Q\bar{Q}$ bound state and allow each gluon line to go soft individually. The soft line is cut, and the cut ends of the long wavelength line are allowed to propagate into the vacuum yielding the set of diagrams illustrated by Fig. 2. Note that the complete set of diagrams of Fig. 2 is exactly the set of diagrams considered by Peskin [2] in determining the gauge invariant coupling of long wavelength gluons to a color singlet heavy $Q\bar{Q}$ bound state. These long wavelength gluons which are coupled to the $Q\bar{Q}$ pair propagate into the vacuum and are "eaten" by a gluon non-zero vacuum expectation value. Note that this procedure is equivalent to allowing the vacuum to have non-zero values for the gauge fields (as given by the vacuum expectation values), and then asking how the $Q\bar{Q}$ system behaves in the presence of this "external" field.

II. Non-perturbative corrections to the color singlet potential

One can easily sum the diagrams of Fig. 2 as Peskin has done [2], using the techniques we reviewed in Chapter I. The well known result gives the first term in an operator product

expansion

$$\text{(Fig. 2)} = \frac{1}{6}\langle\Phi|r^i\frac{1}{H_8 - H_1}r^j|\Phi\rangle\langle 0|g^2G_a^{i0}G_a^{j0}(0)|0\rangle$$

$$+ \frac{1}{24m_Q^2}\langle\Phi|\sigma^i\frac{1}{H_8 - H_1}\sigma^j|\Phi\rangle\langle 0|g^2G_a^{kl}G_a^{mn}(0)|0\rangle\frac{\varepsilon^{ikl}}{2}\frac{\varepsilon^{jmn}}{2} \tag{3.2}$$

where r_i is the $Q\bar{Q}$ separation in the bound state Φ, $H_1(H_8)$ is the Hamiltonian of the $Q\bar{Q}$ in a color singlet (octet) state, $\underset{\sim}{\sigma}$ is the Pauli spin matrix, and the gluon field strength, $G_a^{\mu\nu}$, is evaluated at the origin of the bound state. It should be obvious where the terms in Eq. 3.2 come from. The first term corresponds to the Φ state coupling to the gluon field via an electric dipole interaction, propagating in a color octet state, and then going back to a color singlet Φ state via a second electric dipole interaction. The gluon fields which are coupled to the $Q\bar{Q}$ state are "eaten" by the vacuum, i.e. they're color electric fields which persist independently in the vacuum. The second term in Eq. 3.2 is similar to the first except that the multipole coupling is a magnetic dipole, and the vacuum field is a color magnetic field.

The energy denominator of Eq. 3.2 can be further simplified by noting that for one gluon exchange $H_8 - H_1 = \frac{3g^2}{8\pi r}$. By defining $E_a^i \equiv G_a^{oi}$ and $B_a^i \equiv \frac{1}{2}\varepsilon^{ijk}G^{jk}$, and choosing Φ to be a spin zero state, the expression simplifies to

$$\text{(Fig. 2)} = \frac{\langle\Phi|r^3|\Phi\rangle}{27\alpha_s}\langle 0|g^2\underset{\sim}{E}^a\cdot\underset{\sim}{E}^a|0\rangle$$

$$+ \frac{\langle\Phi|r|\Phi\rangle}{9\alpha_s m_Q^2}\langle 0|g^2\underset{\sim}{B}^a\cdot\underset{\sim}{B}^a|\ \rangle\ . \tag{3.3}$$

Shifman et. al. have determined the vacuum expectation value of the square of the gluon field strength tensor from remarkably successful charmonium sum rules [3]. They find

$$\frac{g^2}{4\pi^2} < 0|G^a_{\mu\nu} G^{\mu\nu}_a|0 > \equiv M_o^4 \approx (330 \text{ MeV})^4 \tag{3.4}$$

which implies (see Appendix A)

$$\frac{g^2}{\pi^2} < 0|\underline{B}^a \cdot \underline{B}^a|0 > = -\frac{g^2}{\pi^2} < 0|\underline{E}^a \cdot \underline{E}^a|0 > = M_o^4 \ . \tag{3.5}$$

We can now rewrite Eq. 3.3 as

$$\text{(Fig. 2)} = h^E + h^M \tag{3.6a}$$

with

$$\begin{aligned} h^E &\equiv -\frac{< \phi|r^3|\phi >}{27\alpha_s} \pi^2 M_o^4 \\ h^M &\equiv \frac{< \phi|r|\phi >}{9\alpha_s m_Q^2} \pi^2 M_o^4 \ . \end{aligned} \tag{3.6b}$$

To determine how this long wavelength "vacuum gluon condensate" affects the bound state Hamiltonian, we will calculate the bound state propagator of the $Q\bar{Q}$ system as illustrated by Fig. 3.

$$\begin{aligned} \text{(Fig. 3)} = \lim_{T \to \infty} \int_0^T dt\, e^{-i(H_1 - \epsilon_1)t} &\left\{ 1 + \int_0^t i dt_1 h^E + \ldots \right\} \\ &\times \left\{ 1 + \int_0^t i dt_1 h^M + \ldots \right\} \end{aligned} \tag{3.7}$$

with ϵ_1 the color singlet bound state energy. Using the identity

$$\int_0^t idt_1 A \int_0^{t_1} idt_2 A \ldots \int_0^{t_{n-1}} idt_n A = \frac{(itA)^n}{n!} \tag{3.8}$$

We can exponentiate the contributions of h^E and h^M to find the corrections to the color singlet Hamiltonian

$$H_1^{s=0} \rightarrow H_1^{s=0} = -\frac{4\alpha_s}{3r} - \left(\frac{\pi^2 M_o^4}{9\alpha_s m_Q^2}\right) < \phi | r | \phi > + \left(\frac{\pi^2 M_o^4}{27\alpha_s}\right) < \phi | r^3 | \phi > \tag{3.9a}$$

for the spin zero bound state. Going back to Eq. 3.2, we can do similar manipulations for the spin one bound state, yielding

$$H_1^{s=1} \rightarrow H_1^{s=1} = -\frac{4\alpha_s}{3r} - \left(\frac{\pi^2 M_o^4}{27\alpha_s m_Q^2}\right) < \phi | r | \phi > + \left(\frac{\pi^2 M_o^4}{27\alpha_s}\right) < \phi | r^3 | \phi > \quad . \tag{3.9b}$$

Note that the second terms in Eqs. 3.9 which result from the magnetic dipole coupling give a "hyperfine" splitting between the s = 0 and s = 1 states.

Equations 3.9a and 3.9b give the leading non-perturbative corrections to the one gluon exchange color coulomb potential. It bears repeating that these expressions are only valid as long as the non-perturbative corrections are small compared to the color coulomb interaction energy, i.e. for sufficiently large m_Q (small r).

III. Results

We are now in a position to determine when the coulombic approximation is a valid one for a given quark mass, and a specified energy level. First note that the "magnetic" term proportional to $<\phi|r|\phi>$ is always much less than the "electric" term proportional to $<\phi|r^3|\phi>$, for $\alpha_s < 1$. Thus, to determine when the coulomb approximation is valid, we can define the ratio

$$R \equiv \frac{\left(\frac{\pi^2 M_o^4}{27\alpha_s}\right)<\phi|r^3|\phi>}{<\phi\left|\frac{4\alpha_s}{3r}\right|\phi>} \tag{3.10}$$

which is the ratio of the energy of the non-perturbative power corrections to the color coulomb binding energy. If $R \ll 1$, the state ϕ can be well described by a coulombic wavefunction. In Fig. 4 we plot R as a function of quark mass for the n = 1, 2, 3 levels of the coulomb spectrum. The coupling constant in the expression for R is normalized to be $\alpha_s = .3$ for $m_Q = 1.5$ GeV, as determined from potential model fits to charmonium [4], and its scale is the bound state Bohr radius, which goes as $(\alpha_s m_Q)^{-1}$. If, for example, we decided that $R < .2$ implies a reasonable color coulomb dominance, the 1s level would be coulombic for $m_Q \geq 10$ Gev, the 2p levels for $m_Q \geq 50$ GeV, the 2s level for $m_Q \geq 60$ GeV, etc. Note that the results are roughly consistent with the crude estimate of Eq. 3.1.

Thus we see that one gluon exchange dominance occurs for quark masses substantially larger than present energies. This is

as expected from the simple estimate of Eq. 3.1, but our new estimates are much more quantitative with a firm theoretical foundation.

IV. Estimate of accuracy of predictions

Two points much be addressed. The first is a guess of the size of the contribution from possible higher dimensional operators in the operator product expansion. Secondly, we must determine how the uncertainty in the experimentally determined quantity, M_o, affects our results.

A. Higher dimensional operators

Dimensionally, we expect higher order operators such as $D_\mu G^a_{\mu\alpha} D_\nu G^a_{\nu\alpha}$, $f^{abc} G^a_{\mu\nu} G^b_{\nu\sigma} G^c_{\sigma\mu}$, etc. to contribute to Eq. 3.2. These should also have non-zero vacuum expectation values since they are Lorentz and color invariants. It is conjectured that the vacuum expectation values of these higher dimensional operators merely occur with appropriate higher powers of M_o, the scale of the vacuum fluctuations. Then, higher dimensional operators contribute in an expansion of $(M_o a_o)$, where a_o is the bound state Bohr radius and originate in the dipole type coupling. This effective expansion parameter is on the order of .15 for $m_Q \sim 20$ GeV, and decreases as $1/m_Q$. Thus the neglect of higher dimensional operators seems quite reasonable.

B. Uncertainty in M_o

Shifman et. al. estimate that $(M_o)^4$ is known to within a factor of two from their sum rules. Shifting the normalization of our curves for R in Fig. 4 by a factor of two induced an uncertainty in our determination of m_Q of roughly ±25%.

Therefore, we see that the calculation is relatively clean, with the experimentally required parameters known to an acceptable accuracy. Since the calculated quark masses where the color coulomb potential dominates are above presently accessible energies, our phenomenological inferences are limited. However, if the top quark and toponium are found, our results tell us that since m_t must be greater than 10 GeV, we expect the wave function at the origin for the lowest lying state to be given by the coulomb wavefunction. This prediction can be checked by measuring the $(t\bar{t})$ branching ratio to charged leptons.

Appendix

A. Non-perturbative techniques of Shifman, Vainshtein, and Zakharov [1]

1. Introduction

Asymptotic freedom allows QCD calculations to be done at short distances since the effective coupling constant of the theory becomes small, insuring a sensible perturbative expansion. However, a complete theory must also include large-distance dynamics as well. What is needed in QCD is a quantitative framework in which to calculate large-distance phenomena. This is the subject of the work of Shifman, Vainshtein, and Zakharov that will now be reviewed.

The central objects studied are the power term corrections to the slowly varying logarithmic terms of perturbative QCD. These power terms are due to non-perturbative effects which limit asymptotic freedom calculations as one tries to extend the short-distance approach to larger distances. Phenomenologically, the power corrections are introduced via non-zero vacuum expectation values (VEV) of gauge invariant field operators such as

$$< 0|G^a_{\mu\nu}G^a_{\mu\nu}|0 > \neq 0 \quad \text{and} \quad < 0|\bar{q}q|0 > \neq 0$$

where q is the quark field and $G^a_{\mu\nu}$ is the gluon field strength tensor. They would vanish by definition in perturbation theory. By giving these operators non-zero VEV's we will see how they induce power corrections to short distance phenomena.

2. Gross features of procedure

Consider a gluon line within a Feynman diagram. (Any type of

line within the diagram would be treated analogously). However, assume the line to be the exact gluon Green function $\mathcal{D}_{\mu\nu}(k^2)$. Splitting $\mathcal{D}_{\mu\nu}(k^2)$ into two parts yields

$$\mathcal{D}_{\mu\nu}(k^2) = \frac{g_{\mu\nu}}{k^2} + \left(\mathcal{D}_{\mu\nu}(k^2) - \frac{g_{\mu\nu}}{k^2} \right)$$

where we work in Feynman gauge for definiteness. As $k^2 \to \infty$, $\mathcal{D}_{\mu\nu}(k^2)$ is given by the first term due to asymptotic freedom. We assume the bracketed term falls off as some power of k^2 as $k^2 \to \infty$. To get the complete answer for the Feynman diagram of interest, we must include both terms in the k^2-integration. The first term is absorbed in the standard perturbative treatment, but the second term gives something new. Since $\left(\mathcal{D}_{\mu\nu}(k^2) - g_{\mu\nu}/k^2 \right)$ is presumably large only for small k^2, we can expand this additional contribution to the amplitude in k^2 and approximate $k^2 = 0$. In the expansion, we must be careful to extract the gluon field strength tensor, $G^a_{\mu\nu} G^a_{\mu\nu}$, so as not to violate gauge invariance.

Doing the k^2-integration results in a number which is sensitive to the gluon dynamics at large distances. If we had a complete theory of confinement, this could be evaluated. In the absence of this, a new parameter is introduced which is equivalent to the vacuum expectation value $< 0 | G^a_{\mu\nu} G^a_{\mu\nu} | 0 >$. This procedure allows us to study non-perturbative effects in simple Feynman diagrams. Note that this is only feasible if all the lines except one are far off-shell and thus known.

3. Example calculation

Consider the T-product of two currents for large external

three-momentum q. For this kinematic regime, it is clear that the operator product expansion [5] is valid. Restricting ourselves to the current $j_\mu = \bar{q}\gamma_\mu q$ in the imaginary world of one quark flavor, and assuming conventional $SU(3)_{color}$, it is an easy exercise to find

$$i\int d^4x\, e^{iqx}\, T\left\{ j_\mu(x) j_\nu(0)\right\} = (q_\mu q_\nu - q^2 g_{\mu\nu}) \times \left\{ -\frac{1}{4\pi^2}\left(1 + \frac{\alpha_s}{\pi}\right) \ln\frac{Q^2}{\mu^2} + \frac{2m_q}{Q^4}(\bar{q}q) + \frac{\alpha_s}{12\pi Q^4} G^q_{\mu\nu} G^a_{\mu\nu} - \frac{2\pi\alpha_s}{Q^6}(\bar{q}\gamma_\alpha \gamma_5 t^a q)(\bar{q}\gamma_\alpha \gamma_5 t^a q) - \frac{4\pi\alpha_s}{9Q^6}(\bar{q}\gamma_\alpha t^a q)(\bar{q}\gamma_\alpha t^q) + \ldots \right\} \tag{A.1}$$

where $Q^2 = -q^2$. For simplicity, we rewrite this expression as

$$^{iqx}\, T\left\{ j_\mu(x) j_\nu(0)\right\} = (q_\mu q_\nu - q^2 g_{\mu\nu})\left(C_I I + C_M \bar{\Psi}\Psi + C_G G^a_{\mu\nu} G^a_{\mu\nu} + C_\Gamma \bar{\Psi}\Gamma\Psi\bar{\Psi}\Gamma\Psi + \ldots \right) . \tag{A.2}$$

When one takes the vacuum expectation values of Eq. A.2, one obtains the photon polarization operator that is used in calculating the rate of e^+e^- going to this particular quark flavor. Note that with the standard perturbative vacuum, only the unit operator would contribute as all others vanish, but by postulating $<0|\bar{\Psi}\Psi|0> \neq 0$,

$< 0|G^a_{\mu\nu} G^a_{\mu\nu}|0 > \neq 0$, etc., there are additional contributions to the polarization tensor.

Defining

$$\pi_{\mu\nu}(Q^2) = (q_\mu q_\nu - q^2 g_{\mu\nu})\pi(Q^2), \tag{A.3}$$

we can take the vacuum expectation value of Eq. A.1 to get

$$\pi(Q^2) = -\frac{1}{4\pi^2}\left[1 + \frac{\alpha_s}{\pi}\right] \ln \frac{Q^2}{\mu^2} + \frac{2}{Q^4} < 0|m_q \bar{q}q|0 > \tag{A.4}$$

$$+ \frac{1}{12\pi Q^4} < 0|\alpha_s G^a_{\mu\nu} G^a_{\mu\nu}|0 > + 0\left(\frac{1}{Q^6}\right) .$$

where only the first few terms are written. Note that this expression is calculable in QCD for Q larger than the scale of the vacuum expectation values.

We also have the general dispersion relation

$$\pi(Q^2) = \frac{1}{\pi}\int \frac{\text{Im } \pi(s) ds}{s + Q^2} \tag{A.5}$$

where Im $\pi(s)$ is proportional to the measurable cross section for e^+e^- annihilation into hadrons with this particular quark flavor content. Equating Eq. A.4 and Eq. A.5 gives a sum rule relating the QCD vacuum expectation values to the integrated experimentally determined e^+e^- hadronic cross section. This is the basic result of Ref. 1. A further technical point is that the information available from this sum rule can be optimized by doing a Borel transformation of both expressions for the polarization operator.

Using these techniques, Shifman et. al. [3] determine from

e^+e^- → charm data

$$\langle 0|\frac{\alpha_s}{\pi} G^a_{\mu\nu} G^a_{\mu\nu}|0\rangle = (330\ \text{MeV})^4 \quad . \tag{A.6}$$

Using different processes, all of the vacuum expectation values can be "measured" in principle, and used to make theoretical predictions for other processes.

4. The $\underset{\sim}{E}_a$ and $\underset{\sim}{B}_a$ vacuum fields

Equation A.6 can be rewritten in terms of $\underset{\sim}{E}_a$ and $\underset{\sim}{B}_a$ fields. This is useful because the two fields have markedly different effects on a heavy quark system. (The E1 and M1 couplings have quite different effective strengths). Demanding that $|\underset{\sim}{E}_a|^2$ and $|\underset{\sim}{B}_a|^2$ have independent Lorentz invariant values puts a restriction on their relative magnitudes. Under a boost with velocity $\underset{\sim}{\beta}$ [6]

$$\begin{aligned} \underset{\sim}{E}^a &\longrightarrow \gamma\left(\underset{\sim}{E}^a + (\underset{\sim}{\beta} \times \underset{\sim}{B}^a)\right) - \frac{\gamma^2}{\gamma+1}\,\underset{\sim}{\beta}(\underset{\sim}{\beta}\cdot\underset{\sim}{E}^a) \\ \underset{\sim}{B}^a &\longrightarrow \gamma\left(\underset{\sim}{B}^a - (\underset{\sim}{\beta} \times \underset{\sim}{E}^a)\right) - \frac{\gamma^2}{\gamma+1}\,\underset{\sim}{\beta}(\underset{\sim}{\beta}\cdot\underset{\sim}{B}^a) \quad . \end{aligned} \tag{A.7}$$

To have $|\underset{\sim}{E}^a|^2$ and $|\underset{\sim}{B}^a|^2$ invariant, $\underset{\sim}{E}_a = \pm i\underset{\sim}{B}_a$. This means $|\underset{\sim}{E}_a|^2 = -|\underset{\sim}{B}_a|^2$. (Note that this is consistent with the fact that even though $\langle G^2\rangle_0 \neq 0$, we want the vacuum energy density to equal zero.) Using this requirement with Eq. A.6 gives

$$\frac{g^2}{\pi^2}\langle 0|\underset{\sim}{B}^a\cdot\underset{\sim}{B}^a|0\rangle = -\frac{g^2}{\pi^2}\langle 0|\underset{\sim}{E}^a\cdot\underset{\sim}{E}^a|0\rangle = (330\ \text{MeV})^4 \quad . \tag{A.8}$$

References and Footnotes

1. M.A. Shifman, A.I. Vainshtein, and V.I. Zakharov, Nucl. Phys. B147 (1979) 385.

2. M.E. Peskin, Nucl Phys1 B156 (1979) 365.

3. M.A. Shifman, A.I. Vainshtein, and V.I. Zakharov, Nucl. Phys. B147 (1979) 448.

4. G. Bhanot and S. Rudaz, Phys. Lett. 78B (1978) 119.

5. K. Wilson, Phys. Rev. 179 (1969) 1499.

6. J.D. Jackson, Classical Electrodynamics, J. Wiley and sons, New York, 1975.

Figure Captions

Fig. 1 Lowest order perturbative diagrams for gluon exchange within a $Q\bar{Q}$ bound state.

Fig. 2 Sum of diagrams generated by cutting the soft gluon lines of Fig. 1.

Fig. 3 Vacuum gluon condensate contribution to the $Q\bar{Q}$ propagator.

Fig. 4 The quantity R, as defined in Eq. 3.10, as a function of m_Q for the n = 1, 2, 3 levels of the coulomb spectrum.

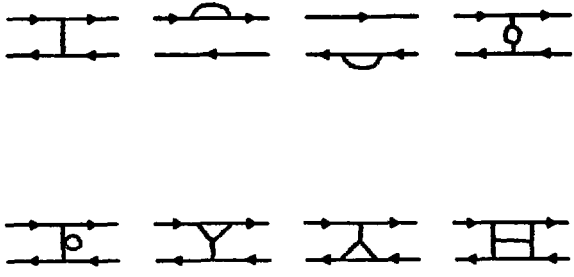

FIG. 1

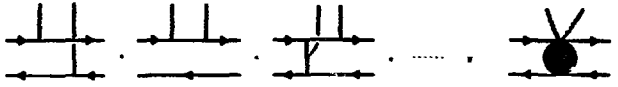

FIG. 2

FIG. 3

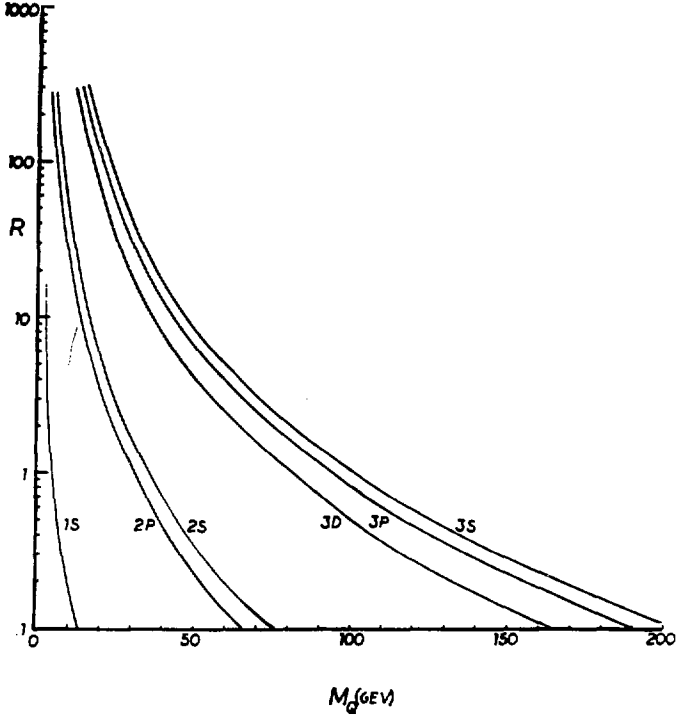

FIG. 4

CHAPTER IV

Non-perturbative Calculation of the Heavy Quark Potential

Abstract

Non-perturbative contributions are incorporated into the heavy quark potential via non-zero vacuum expectation values of gauge invariant operators à la Shifman, Vainshtein, and Zakharov. The derived potential exhibits the appropriate short distance 1/r behavior and the asymptotic linear confining potential. The calculated coefficient of the linear term is in striking agreement with phenomenological potentials that are constructed to reproduce the heavy quarkonia spectra, and gives the proper Regge slope.

I. Introduction

The $Q\bar{Q}$ color singlet potential will be calculated by including two contributions —— the one gluon exchange potential and the induced potential from a non-zero vacuum expectation value of the operator $g^2 G^a_{\mu\nu} G^{\mu\nu a}$. Intuitively speaking, the problem of including the effects of this non-perturbative vacuum gluon condensate is equivalent to solving the process under consideration in constant uniform color electric and magnetic fields. Of course, the contributions of higher dimensional and possibly non-uniform vacuum fields must also be considered, and either included or shown to be negligible for the relevant process. The effect of this gluon condensate on the quark-antiquark potential can be evaluated quite simply using multipole techniques. The justification for this procedure is that as long as the size of the vacuum gluon fluctuations is larger than the size of the $Q\bar{Q}$ system, the expansion parameter $(\underset{\sim}{k}\cdot\underset{\sim}{r})$ is a small number. Since the vacuum condensate is effectively spatially homogeneous, a lowest order multipole expansion can be used out to relatively large distances. Of course, higher multipoles which couple to gradients of the vacuum fields could contribute when deviations from the homogeneous approximation are incorporated. However, as will be pointed out, these are unimportant out to a distance of roughly a fermi.

The reason that this calculation is valid out to distances where the non-perturbative effects dominate while the results of Chapter III are only valid when non-perturbative effects are small, is that here we will sum the non-perturbative contributions to all

orders via a non-linear equation. We can then estimate the size of the neglected contributions, and will show that these are negligible out to quite large distances.

II. Calculation of H_1 as a function of H_β

The derivation begins by allowing a static $Q\bar{Q}$ pair which is in a color singlet state and interacting via a one gluon exchange potential to couple an arbitrary number of times to a vacuum field, as in Fig. 1. (The static $m_Q \to \infty$ condition will be relaxed in Sec. VI, allowing spin coupling terms.) As is known from the one gluon exchange potential, the intermediate color octet $Q\bar{Q}$ states are in a repulsive channel, and thus highly virtual with respect to the color singlet incident state (see Chapter I, Appendix B). Thus, the vacuum couplings clump into short periods of octet propagation, separated by longer periods of color singlet propagation [1]. Furthermore, the vacuum only contains the color singlet combination $G^a_{\mu\nu}G^{\mu\nu a}$ and pairs of gluon indices must be contracted. Figure 2 results from this reduction of Fig. 1.

The two particle irreducible interaction kernel which describes the vacuum contribution to the color singlet propagation is chosen to be of the form given by Fig. 3a. One should notice at this point that the form of the 2PI interaction kernel has been restricted by the choice of Fig. 3a. The restriction is that the vacuum couples to the $Q\bar{Q}$ pair in a nested series of "rainbow" diagrams. This is a feature of the calculation that is necessary for computational reasons, since the combinatoric problems associated with non-rainbow diagrams appear to be insurmountable.

This approximation is not without justification however, since the non-rainbow diagrams are non-planar, and suppressed by $1/N_c$ to each order in the non-planarity. This is a general result for diagram topologies [2], and easily verified to lowest order for this process.

Another important feature to notice about the 2PI interaction kernel of Fig. 3 is that the color octet Hamiltonian, H_8', that appears is not a complete physical Hamiltonian. It contains the one gluon exchange diagrams and coupling to the vacuum fields with the restriction that the $Q\bar{Q}$ pair remains in a color octet state at all times, with no intermediate color singlet states. This is an obvious requirement as can be seen by reexamining Fig. 2 and recalling that the color singlet states tend to propagate for long time periods. This singlet propagation would destroy the localization in time necessary to couple to the vacuum field, which is bilinear at a space-time point. Similarly, Fig. 3b describes the vacuum contribution to the color octet state propagation, with the same restriction to color octet intermediate states.

When iterated, these 2PI kernels can be used to solve for the full color singlet Hamiltonian which includes one gluon exchange and the vacuum condensate contributions. Figure 3a gives

$$\text{(Fig. 3a)} \;= (-iH_I)\int_0^\infty d\tau\, e^{-i\tau(H_8' - H_1^o)}\,(-iH_I)dt$$

$$= H_I \frac{1}{(H_8' - H_1^o)} H_I\, idt \qquad (4.1)$$

where H_I is the gluon-quarkonium interaction Hamiltonian, H_8' is the complete (but non-physical, as discussed) color octet Hamiltonian, and H_1^o is the one gluon exchange color singlet Hamiltonian. Making the definition

$$\text{(Fig. 3a)} \equiv i h_1^E \, dt \ ,$$

we can iterate Fig. 3a to find the full color singlet propagator

$$\lim_{T \to \infty} \int_0^T dt \, e^{-i(H_1 - i\varepsilon)t} = \lim_{T \to \infty} \int_0^T dt \, e^{-i(H_1^o - i\varepsilon)t} \times \left\{ 1 + \int_0^t i dt_1 h_1^E + \ldots \right\}$$

$$= \lim_{T \to \infty} \int_0^T dt \, e^{-i(H_1^o - h_1^E - i\varepsilon)t} \ .$$

This gives

$$H_1 = H_1^o - h_1^E$$

$$= -\frac{4\alpha_s}{3r} - H_I \frac{1}{H_8' - H_1^o} H_I \ . \qquad (4.2)$$

To solve Eq. 4.2 for H_1 one must know the form of H_I, the gluon-quarkonium coupling. As stated before, the coupling of the uniform vacuum field to the $Q\bar{Q}$ pair suggests a lowest order multipole interaction. The form of this interaction has been derived by

several authors [3], and is given by

$$\mathcal{L}_I = \sum_a \left[- \iota_a A_a^o(0,t) + \underset{\sim}{d}_a \cdot \underset{\sim}{E}_a(0,t) + \underset{\sim}{m}_a \cdot \underset{\sim}{B}_a(0,t) + \ldots \right] \tag{4.3}$$

where

$$\begin{aligned} Q_a &= g \int d^3r\, \bar{\Psi} \gamma_o T_a \Psi \\ \underset{\sim}{d}_a &= g \int d^3r\, \underset{\sim}{r}\, \bar{\Psi} \gamma_o T_a \Psi \\ \underset{\sim}{m}_a &= g \int d^3r\, \frac{1}{2} (\underset{\sim}{r} \times \bar{\Psi} \underset{\sim}{\gamma} T_a \Psi) \end{aligned} \tag{4.4}$$

with Ψ the $Q\bar{Q}$ wavefunction, $\underset{\sim}{r}$ the $Q\bar{Q}$ separation, and T_a the generators of $SU_c(3)$. Using this interaction in the static quark ($m_Q \to \infty$) limit, Eq. 4.2 becomes

$$H_1 = - \frac{4\alpha_s}{3r} - \frac{1}{18} r^2 \frac{i}{\left(H_8' + \frac{4\alpha_s}{3r} \right)} < 0 | g^2 \underset{\sim}{E}_a^2 | 0 > \quad . \tag{4.5}$$

To complete the calculation, we must calculate H_8'.

III. Calculation of H_8'

The determination of H_8' follows exactly the same procedure as that of H_1, except using the iteration of the 2PI kernel given by Fig. 3b rather than Fig. 3a. However, there is one subtle point that may be missed by just forging ahead with the naive manipulations. That point is the elimination of a potential infra-red problem in the determination of H_8'. This can be seen by looking at the lowest order graph contained in the 2PI kernel for H_ρ', as given

by Fig. 4. For the gluon momentum going to zero (homogeneous field approximation), the energy denominator for the gluon-$Q\bar{Q}$ vertex develops a zero, since the energy of the system has not been changed by the interaction. However, this singularity is eliminated by including the full (but non-physical) color octet Hamiltonian for the $Q\bar{Q}$ propagator inside the rainbow diagram as in Fig. 3b. That this is in fact the correct procedure can be seen by looking at the lowest order iterations of the 2PI kernel of Fig. 3b in the calculation of the Hamiltonian, H_8'. This is given by Fig. 5. Here, of course, we have a non-zero energy denominator across each vertex. Including potentially infra-red singular diagrams such as Fig. 6 would be overcounting, since this diagram is already a part of the expansion of Fig. 5.

Now, H_8' can be determined in exactly the same fashion as H_1. Analogous to Eq. 4.2, we find

$$H_8' = H_8^o - H_I \frac{1}{H_8' - H_8^o} H_I \tag{4.6}$$

where H_8^o is the one gluon exchange potential in the color octet state. Using the form of H_I given in Eq. 4.3 and Eq. 4.4, and the form of H_8^o derived in Appendix B of Chapter I we find

$$H_8' = \frac{\alpha_s}{6r} - \frac{5}{288} r^2 \frac{1}{(H_8' - \frac{\alpha_s}{6r})} < 0|g^2 E_a^2|0 > . \tag{4.7}$$

IV. Solution for H_1

Equation 4.7 can be used to solve for H_8' algebraically in terms of known quantities and variables, and then substituted into Eq. 4.5

to find the final expression for the color singlet potential. Using Eq. 3.5 of Chapter III for the vacuum expection value of E_{-a}^2, we find

$$H_1 = -\frac{4\alpha_s}{3r} + \frac{\pi^2 M_o^4 r^2}{18\left(\frac{3\alpha_s}{2r} + \sqrt{\frac{5}{288}}\,\pi M_o^2 r\right)} \quad . \tag{4.8}$$

This is the primary result of this work. The interesting features of this derived potential are that it has the expected coulomb-like behavior $\sim -\frac{4\alpha_s}{3r}$ at short distances, and a linearly rising potential for large r,

$$H_1 \xrightarrow[r \text{ large}]{} \frac{2\pi M_o^2}{3}\sqrt{\frac{2}{5}}\; r \quad . \tag{4.9}$$

Numerically, the long distance potential is

$$H_1 \xrightarrow[r \text{ large}]{} (.144 \text{ GeV}^2)\; r \quad . \tag{4.10}$$

It is interesting to compare the coefficient of the linearly rising term with phenomenological potentials that have been fit to the heavy quarkonia data. Fitting the upsilon spectrum to a coulomb plus logarithmic plus linear potential [4] gives

$$H_1^{exp} \xrightarrow[r \text{ large}]{} (.155 \text{ GeV}^2)\; r \quad . \tag{4.11}$$

If one demands that the phenomenological potential reproduces a Regge slope of .9 GeV^{-2}, one finds

$$H_1^{exp} \xrightarrow[r \text{ large}]{} \frac{r}{2\pi\alpha'} \longrightarrow (.143\ GeV^2)r \quad . \tag{4.12}$$

There is spectacular agreement between our derived potential and these phenomenological potentials inferred from the data. Our potential however, has an analytic interpolating form between the previously conjectured long distance linear confining potential and the short distance coulomb-like potential. Detailed calculations of the quarkonium spectra using the potential of Eq. 4.8 are forthcoming.

V. Spin coupling terms

There also exist terms which couple the vacuum magnetic field to the quark spins. Since the magnetic dipole coupling $\left(\sim \frac{\underline{\sigma}\cdot\underline{B}}{2m_Q}\right)$ is smaller than the electric dipole coupling ($\sim \underline{r}\cdot\underline{E}$) for large m_Q, we will treat the magnetic terms as a perturbation in $1/m_Q$. Doing the same manipulations as in Sec. II, but including the magnetic dipole couplings along with the electric dipole couplings leads to a modified Eq. 4.2

$$H_1 = -\frac{4\alpha_s}{3r} - H_I^E \frac{1}{H_8' - H_1^o} H_I^E - H_I^M \frac{1}{H_8' - H_1^o} H_I^M \quad .$$

Using Eq. 4.3 for the specific form of H_I^E and H_I^M, and also carefully taking into accout the $Q\bar{Q}$ spin structure since H_I^M is

spin dependent, we find

$$H_1 = -\frac{4\alpha_s}{3r} - \frac{1}{18} r^2 \frac{1}{\left(H_8' + \frac{4\alpha_s}{3r}\right)} < 0|g^2 \underset{\sim}{E}_a^2|0 > \\ - \frac{1}{6m_Q^2} \frac{\left[1 - \frac{1}{3} s(s+1)\right]}{\left(H_8' + \frac{4\alpha_s}{3r}\right)} < 0|g^2 \underset{\sim}{B}_a^2|0 > \tag{4.13}$$

where s is the total spin of the $Q\bar{Q}$ pair. Since the spin dependent terms are only included to lowest order in $1/m_Q$, H_8' is calculated as before by only including electric dipole vacuum couplings. Using the solution of Eq. 4.7 for H_8' as before, we find that H_1 with the inclusion of spin dependent terms becomes

$$H_1 = -\frac{4\alpha_s}{3r} - \frac{\pi^2 M_o^2 r^2}{18\left(\frac{3\alpha_s}{2r} + \sqrt{\frac{5}{288}}\, \pi M_o^2 r\right)} \\ - \frac{\pi^2 M_o^2 \left[1 - \frac{1}{3} s(s+1)\right]}{6m_Q^2\left(\frac{3\alpha_s}{2r} + \sqrt{\frac{5}{288}}\, \pi M_o^2 r\right)} . \tag{4.14}$$

This "color hyperfine" interaction can be used to calculate spin splittings within the heavy quarkonia spectra, for example the $\psi(^3S_1) - \eta_c(^1S_o)$ mass difference. To do this requires solving for the wavefunction using the unperturbed potential of Eq. 4.8, and then calculating the energy difference using the additional hyperfine term of Eq. 4.14. This calculation awaits our

previously mentioned forthcoming numerical work. However, it is of interest to very crudely estimate the $\psi - \eta_c$ mass splitting using the $H_{hyperfine}$.

$$m_\psi - m_{\eta_c} \approx \left\langle \frac{\pi^2 M_o^4}{6m_c^2\left(\frac{3\alpha_s}{2r} + \sqrt{\frac{5}{288}}\,\pi M_o^2 r\right)} \right\rangle \left[-\frac{1}{3} - (-1)\right]$$

$$= \frac{\pi^2 M_o^4}{9m_c^2} \left\langle \frac{1}{\frac{3\alpha_s}{2r} + \sqrt{\frac{5}{288}}\,\pi M_o^2 r} \right\rangle .$$

Just for definiteness, let us assume that this expectation value is dominated by the short distance part of the wavefunction. Then

$$m_\psi - m_{\eta_c} \approx \frac{2\pi^2 M_o^4}{27\alpha_s m_c^2} \langle r \rangle .$$

Using values of $\langle r \rangle = 1.2$ f, $\alpha_s = .41$, and $m_c = 1.6$ GeV from Ref. 5 for the standard charmonium potential of coulomb plus linear terms yields

$$m_\psi - m_{\eta_c} \approx 50 \text{ MeV} .$$

This should only be interpreted as the correct order of magnitude, due to the gross nature of the approximations. A critical test awaits the detailed numerical calculations of the charmonium wavefunction using the potential of Eq. 4.8. However, the preliminary results are very encouraging.

V. Validity of approximations

Two points must be investigated. First of all, the validity of the neglect of higher order multipole terms must be evaluated. The next higher order term that contributes in the expansion of Eq. 4.3 and Eq. 4.4 will be estimated. Secondly, the neglect of other higher dimensional operators that contain higher powers of the quantum fields will be analyzed, i.e. operators that are tri-linear in the gluon field strength tensor, etc.

A. Neglect of higher multipoles

The work of Yan [3] can be expanded to higher order quite simply, yielding for the form of the gluon-heavy quark interaction Lagrangian

$$\mathcal{L}_I = \sum_a \Big[- Q_a A_{o_a}(0,t) + \underset{\sim}{d}_a \cdot \underset{\sim}{E}_a(0,t) + \frac{1}{2!}(\underset{\sim}{x}\cdot\underset{\sim}{\nabla}) \underset{\sim}{d}_a(0,t) + \frac{1}{3!}(\underset{\sim}{x}\cdot\underset{\sim}{\nabla})^2 \underset{\sim}{d}_a \cdot \underset{\sim}{E}_a(0,t) + \ldots + (\text{magnetic terms}) + \ldots \Big]$$

where the definitions are as in Eq. 4.4. The next order term, $\frac{1}{2!}(\underset{\sim}{x}\cdot\underset{\sim}{\nabla})\underset{\sim}{d}_a \cdot \underset{\sim}{E}_a$, does not contribute when summed over quark and antiquark, and the first non-leading term is $\frac{1}{3!}(\underset{\sim}{x}\cdot\underset{\sim}{\nabla})^2 \underset{\sim}{d}_a \cdot \underset{\sim}{E}_a$. A very crude estimate of this term can be made by assuming $(\underset{\sim}{x}\cdot\underset{\sim}{\nabla})^2 \rightarrow (\frac{r}{2})^2 k^2$, where k is the gluon energy. This energy is assumed to be on the scale of the fluctuations of the vacuum condensate, M_o. Therefore, we expect

$$\frac{1}{3!}(\underset{\sim}{x}\cdot\underset{\sim}{\nabla})^2 \underset{\sim}{d}_a \cdot \underset{\sim}{E}_a \longrightarrow \frac{1}{3!}(\frac{r}{2}M_o)^2 \times \text{(lowest order)}.$$

This means the corrected amplitude has the form

$$\left(1 + \frac{.117r^2}{(\text{fermi})^2}\right) \times \text{(lowest order)} \quad .$$

The correction is less than 12% out to a distance of a fermi. Since the bulk of the wavefunction exists within this range, these corrections are expected to be quite small.

B. Neglect of other higher dimensional operators

The next higher dimensional operator that is Lorentz and gauge invariant, and could have a non-zero vacuum expectation value is

$$f_{abc} < 0|G^a_{\mu\nu} G^b_{\nu\alpha} G^c_{\alpha\mu}|0 > \neq 0 \quad .$$

It might be expected to contribute with only one higher power of $(\underset{\sim}{r}\cdot\underset{\sim}{k})$ than lowest order. Note that this is only true for three color electric dipole couplings. However, the form of this matrix element demands that at least one of the fields be a color magnetic field, and thus be down by a power of $1/m_Q$. Therefore, in the static quark approximation the next contributing operator will be quartic in the gluon fields. Dimensionally it is expected to contribute with roughly the same strength as the term in Section A, since it also is suppressed by two powers of the effective expansion parameter.

While originally it may have appeared that our derived potential's spectacular agreement with the phenomenologically motivated potentials was fortuitous, it now appears that the approximations made were in fact very reasonable. The vacuum fields are quite homogeneous, and thus appear effectively uniform out to relatively large distances. The case of uniform fields can be handled quite accurately, giving us very trustworthy results.

References

1. M.E. Peskin, Nucl. Phys. B156 (1979) 365; T. Applequist, M. Dine, and I. Muzinich, Phys. Rev. D17 (1978) 2074.
2. S. Coleman, Proceedings of the International School of Subnuclear Physics, Erice, Italy, July 1979.
3. T.-M. Yan, Phys. Rev. D22 (1978) 1652; K. Shizuya, LBL Report No. LBL-11004 (to be published).
4. G. Bhanot and S. Rudaz, Phys. Lett 78B (1978) 119.
5. M. Krammer and H. Krasemann, DESY Report No. DESY 79/20.

Figure Captions

Fig. 1 Quark-antiquark pair interacting via one gluon exchange, and coupling to the vacuum gluon condensate.

Fig. 2 Clustering of the quarkonium-vacuum field interactions about regions of color octet propagation.

Fig. 3 (a) 2PI kernel describing the vacuum contribution to the color singlet $Q\bar{Q}$ propagator.

(b) 2PI kernel describing the vacuum contribution to the color octet $Q\bar{Q}$ propagator.

Fig. 4 The lowest order term of the color octet 2PI kernel.

Fig. 5 Iteration of the 2PI kernel to generate the $Q\bar{Q}$ propagator.

Fig. 6 A potential infra-red singular term in the iteration of the 2PI kernel to generate the $Q\bar{Q}$ propagator.

FIG. 1

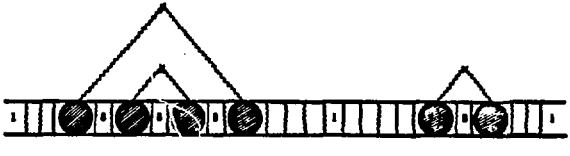

FIG. 2

FIG. 3

FIG. 4

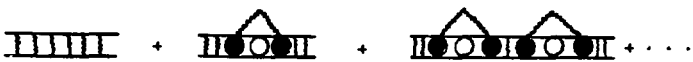

FIG. 5

FIG. 6

Summary

It has been seen that there exist several physically measurable processes that can be reliably calculated using multipole techniques within the framework of heavy quarks and QCD. This is extremely important because of the scarcity of quantitative confrontations between experiment and the conjectured theory. These techniques can be applied to kinematic regimes that are complimentary to standard perturbative calculations, and in fact can be extended into the realm of non-perturbative physics as we saw in Chapters III and IV. The multipole expansion is ideally suited to investigate some manifestations of the long distance infra-red structure of QCD that may ultimately be connected with confinement.

There are several immediate extensions of the work contained in this thesis that could be very useful. The first extension is the numerical calculation of heavy quarkonia spectra using the derived potential of Chapter IV. This will allow immediate confrontation between experiment and theory through comparison to existing ψ and T data Secondly, relativistic corrections to the derived potential can be incorporated through a Bethe-Salpeter formalism. This is useful since the ψ system is believed to have important relativistic corrections, and it would also allow the determination of spin-orbit couplings which could be compared to existing χ-state splittings in the charmonium systems.